



Research paper

Discovery of chalcone analogues as novel NLRP3 inflammasome inhibitors with potent anti-inflammation activities

Cheng Zhang¹, Hu Yue¹, Ping Sun¹, Lei Hua, Shuli Liang, Yitao Ou, Dan Wu, Xinyi Wu, Hao Chen, Ying Hao, Wenhui Hu^{**}, Zhongjin Yang^{*}

Key Laboratory of Molecular Target & Clinical Pharmacology and State Key Laboratory of Respiratory Disease, School of Pharmaceutical Sciences & the Fifth Affiliated Hospital, Guangzhou Medical University, Guangzhou, Guangdong, 511436, China

ARTICLE INFO

Article history:

Received 1 March 2021

Received in revised form

22 March 2021

Accepted 23 March 2021

Available online 1 April 2021

Keywords:

NLRP3 inflammasome

Inhibitor

Michael acceptor

ABSTRACT

NLRP3 inflammasome activation plays a critical role in inflammation and its related disorders. Herein we report a hit-to-lead effort resulting in the discovery of a novel and potent class of NLRP3 inflammasome inhibitors. Among these, the most potent lead **40** exhibited improved inhibitory potency and almost no toxicity. Further mechanistic study indicated that compound **40** inhibited the NLRP3 inflammasome activation via suppressing ROS production. More importantly, treatment with **40** showed remarkable therapeutic effects on LPS-induced sepsis and DSS-induced colitis. This study encourages further development of more potent inhibitors based on this chemical scaffold and provides a chemical tool to identify its cellular binding target.

© 2021 Elsevier Masson SAS. All rights reserved.

1. Introduction

NLRP3 inflammasome is a prospective drug target against inflammation and its related diseases [1]. It is a protein complex in the cytoplasm composed of the inflammasome sensor molecule (NLRP3 protein), the adaptor protein ASC and the effector component (pro-caspase-1) [2]. The activation of NLRP3 inflammasome requires a two-stage process: a priming stage and an activation stage. The priming step is referred to the upregulation of transcription of NLRP3 and prointerleukin-1 β (pro-IL-1 β) through the nuclear factor kappa B (NF- κ B) pathway after pathogen-associated molecular patterns (PAMPs) or damage associated molecular patterns (DAMPs) stimulation of a Toll-like receptor (TLR). In the second activation step, the primed cell is stimulated by a second stimulus (typically a DAMP in sterile inflammation), which causes activation of the NLRP3 inflammasome [3–5]. The activated NLRP3 inflammasome induces pro-caspase-1 self-cleavage into active caspase-1, which further cleaves pro-IL-1 β into mature IL-1 β and releases it into extracellular [6,7].

Increasing evidence shows that NLRP3 inflammasome is closely related to various human diseases, such as peritonitis, colonic inflammation, nonalcoholic steatohepatitis (NASH), and Alzheimer's disease (AD) [8–15]. NLRP3 inflammasome activation involves several mechanisms: intracellular ion flux (such as K⁺ efflux) [16], release of lysosomal resident cathepsin B [17], production of reactive oxygen species (ROS) [18], and ubiquitin/deubiquitination post-translation modification of NLRP3 [19]. Yet there is no unified statement about its main activation mechanism. As shown in Fig. 1, many small molecules showed different levels of inhibitory activities on NLRP3 inflammasome [20–28]. Among these, most inhibitors exhibited a micromolar inhibitory activity. The most potent MCC950 inhibits IL-1 β release with high potency (IC₅₀ in BMDMs: 7.5 nM) and specificity [20]. However, it was not developed as it was found to induce liver toxicity in clinical trials, which may be caused by its metabolically reactive furan moiety or high drug dose of 1200 mg per day [1]. Notably, Somalix (Inflazome's), IFM-2427 (IFM Tre/Novartis's), and NT-0167 (Nodthera's) are currently undergoing phase II or I clinical trials [29]. In addition, another NLRP3 inhibitor OLT1177 (non-dose dependence, IC₅₀: ~0.1 μ M in J744A.1) [21], chemically different from MCC950, is currently undergoing phase II clinical trials for treatment of osteoarthritis, but it is also facing the same test of high-dose drug safety (1000 mg doses of OLT1177 daily) [1]. Therefore, there is still great enthusiasm in seeking novel types of small-molecule inhibitors against NLRP3 inflammasome activation.

* Corresponding author.

** Corresponding author.

E-mail addresses: huwenhui@gzhmu.edu.cn (W. Hu), yzj23@gzhmu.edu.cn (Z. Yang).¹ These authors contributed equally to this work.

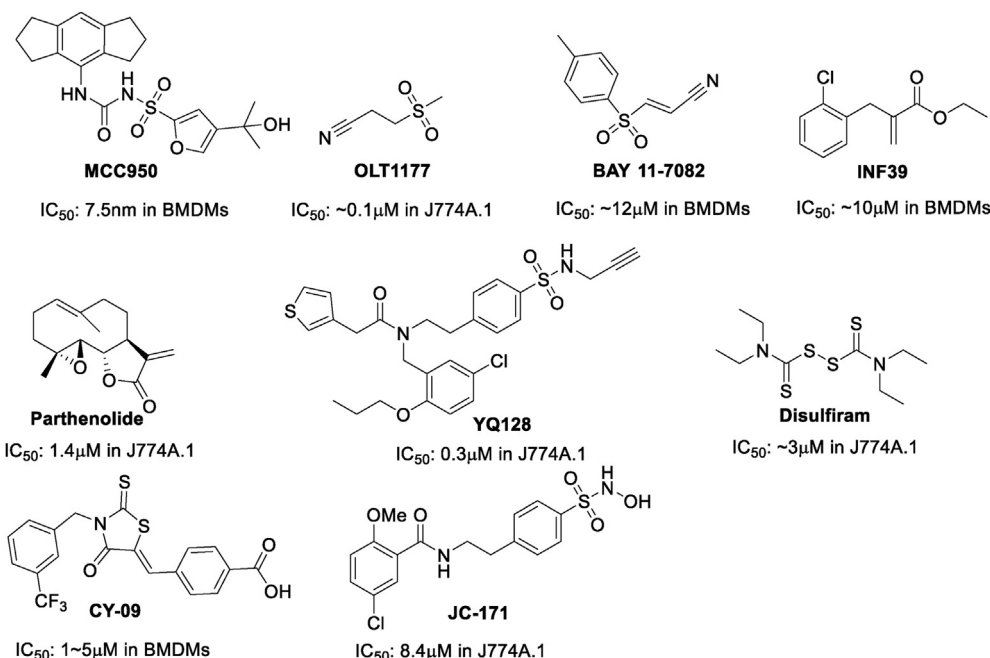


Fig. 1. Compound structures and potency of identified NLRP3 inhibitors.

To address this issue, we screened compounds that are either in clinical use or have reached late-stage clinical trials and identified elafibranor (GFT505) as an inhibitor against IL-1 β release mediated by NLRP3 inflammasome. GFT505, developed by the French company, was a peroxisome proliferation-activated receptor- α/δ (PPAR- α/δ) dual agonist as a drug candidate to treat NASH [30,31]. Unfortunately, in May 2020, it was disclosed to fail to hit the pre-defined primary endpoint of NASH with an improvement of fibrosis, and terminated in a Phase III study. Despite this, the chalcone scaffold was at least proved to possess good safety. In our screening model, GFT505 showed low inhibitory potency toward NLRP3 inflammasome mediated IL-1 β release with IC_{50} of ~40 μ M. In addition, its calculated lipophilicity (cLogP) is high, 5.1. Generally, lower cLogP as well as lower molecular weight (MW) are beneficial to achieve good druggable profiles [32,33]. Another undeniable fact is that lead-to-drug optimization generally tends to raise cLogP and MW. All in all, GFT505 is not yet qualified as a lead compound and requires far more effort to be optimized. Therefore, it is clear to increase its potency while reducing cLogP and MW to make it a suitable lead compound.

Herein, we describe work that leads to the identification of a potent NLRP3 inhibitor for the treatment of inflammation-related diseases. Furthermore, the mechanism of NLRP3 inflammasome inhibition is primarily studied due to its ability to inhibit IL-1 β release from macrophages and to affect the NLRP3 activation. Finally, in vivo pharmacological studies in animal models of sepsis and colitis show relevant therapeutic effects on inflammation.

2. Results and discussion

2.1. Design and synthesis of GFT505 analogues

GFT505 (**1**) includes a pharmacologically active chalcone structure bearing a hydroxyisobutyric acid, methylthiol group, and two methyl groups in positions 4, 4' and 3 (or 5), respectively. Thus, we started a tentative structure-activity relationship (SAR) study and designed an initial set of 14 analogues that were synthesized and tested against NLRP3 inflammasome mediated IL-1 β release

(summarized in Fig. 2: Box A and B). This further systematic SAR exploration led to the final lead compound. The design of compounds **2–15** was mainly to understand the tolerability of bilateral regions to various functional group substitutions. Analogues **16–29** were designed to examine the importance of substituents of phenyl in β position to their biological activities. Then, a further design of compounds **30–40** was to evaluate whether the replacement of methylthiol moiety with various groups could improve biological activity.

The preparation of the designed compounds was achieved by the conditions as described in Scheme 1. Briefly, compounds **2–4**, **16–32** and **35–40** were obtained by the Claisen–Schmidt condensation of substituted acetophenones **1a–i** and benzaldehyde **2a–m**. Treatment of **3** with various isocyanates in toluene at 70 °C gave compounds **5–8** (Scheme 1). Reaction of **17** with the corresponding bromides or propyl isocyanate to afford **10**, **15** or **14**. Compounds **11–13** were synthesized by the substitution reaction of **17** with various bromocarboxylates in the presence of K_2CO_3 followed by hydrolysis. Using different equivalent ratios of *m*-CPBA in CH_2Cl_2 , thioether **17** was oxidized to compounds **33** and **34**, respectively.

2.2. Development of structure-activity relationship (SAR)

A cellular model has been established in our previous study using murine macrophages cell line J774A.1, in which the release of IL-1 β is mediated via the NLRP3 inflammasome upon stimulation with lipopolysaccharide (LPS) and Nigericin [26]. The enzyme-linked immunosorbent assay (ELISA) was used to detect the level of IL-1 β secretion. As shown in Table 1, GFT505 exhibited a relatively weak inhibitory potency with an IC_{50} of 39.6 μ M. The replacement of the 2-carboxyisopropanyl with methyl group (**2**) exhibited slightly diminished inhibitory activity (IC_{50} = 49.5 μ M). In the beginning, considering its facile synthesis, we used compound **2** as a template to study the effect of methylthiol substituent at 4' position on the activity. As shown in Table 1, amino group replacing methylthiol at 4' position (**3**) significantly improved the inhibitory activity with an IC_{50} of 5.7 μ M. Due to the

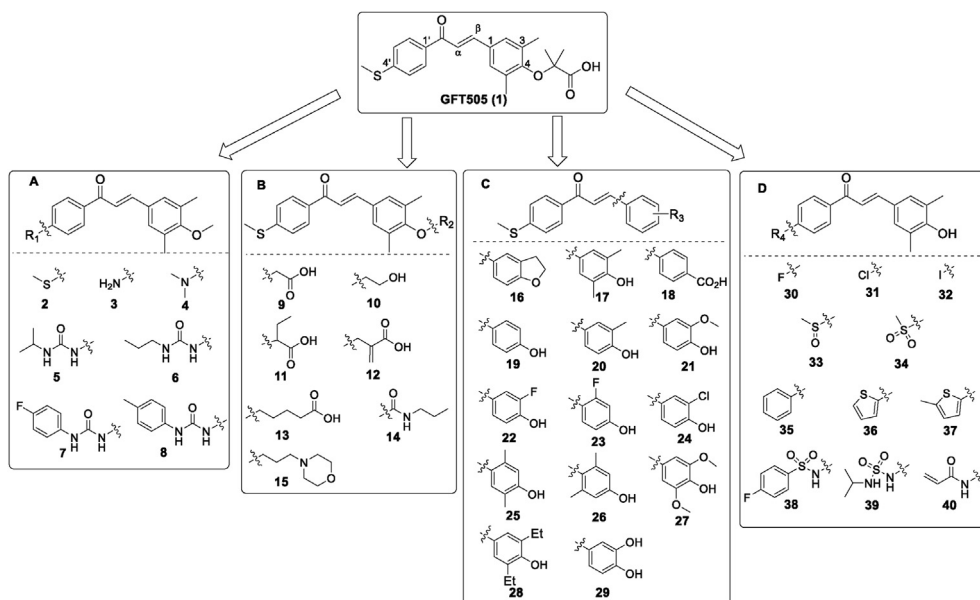
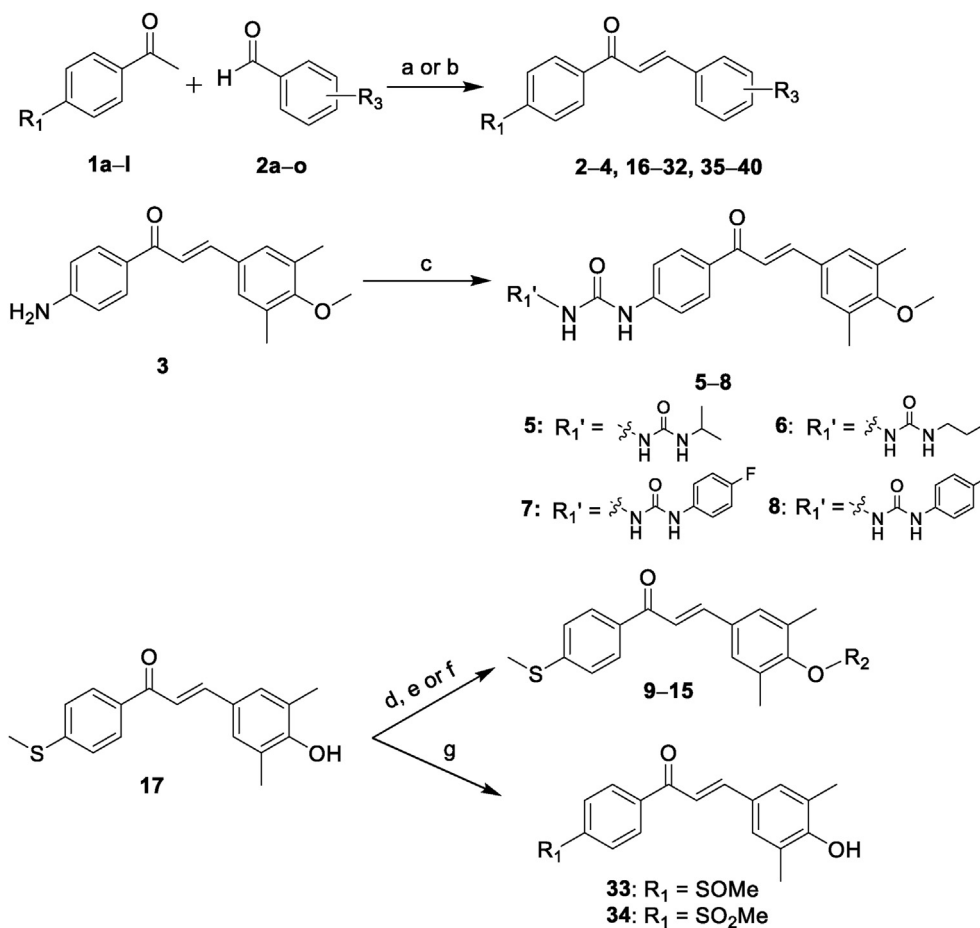
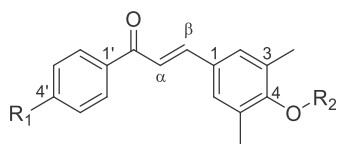


Fig. 2. Chemical structures of the designed analogues of GFT505.



Scheme 1. Chemical synthesis of the designed analogues. Reagents and conditions: (a) 4 M HCl in MeOH, rt, 24 h; (b) NaOH, MeOH, rt, 24 h; (c) various isocyanates, toluene, 70 °C, overnight; (d) various bromides or bromocarboxylates, K₂CO₃, DMF, 90 °C, 6 h; (e) LiOH, THF, H₂O, 50 °C, overnight; (f) propyl isocyanate, TEA, CH₂Cl₂, rt, 5 h; (g) *m*-CPBA (**33**:1.0 eq, **34**: 2.6 eq), CH₂Cl₂, 0 °C or rt, 5 h.

Table 1
Inhibitory potency of analogues 2–15 on IL-1 β release mediated by NLRP3 inflammasome activation in J774A.1 Cells.



Compd	R ₁	R ₂	IC ₅₀ (μ M) ^a	cLogP ^b	LE ^c	LLE ^d
GFT505 (1)	SMe		39.6 \pm 7.5	5.11	0.22	-0.71
2	SMe	Me	49.5 \pm 4.2	5.20	0.27	-0.90
3	NH ₂	Me	5.7 \pm 0.2	3.82	0.34	1.42
4	NMe ₂	Me	25.9 \pm 1.0	5.02	0.27	-0.43
5		Me	33.2 \pm 0.3	4.89	0.23	-0.41
6		Me	9.6 \pm 2.0	5.11	0.25	-0.09
7		Me	23.5 \pm 11.7	6.21	0.20	-1.58
8		-CH ₃	38.7 \pm 4.2	6.46	0.19	-2.05
9	SMe		>40.0	4.49	n.d. ^e	n.d. ^e
10	SMe		12.7 \pm 1.0	4.33	0.28	0.57
11	SMe		31.7 \pm 6.0	5.33	0.23	-0.83
12	SMe		>40.0	5.04	n.d. ^e	n.d. ^e
13	SMe		28.9 \pm 0.1	5.37	0.22	-0.83
14	SMe		22.3 \pm 4.1	4.91	0.25	-0.26
15	SMe		21.9 \pm 2.8	5.63	0.21	-0.97

^a IC₅₀ values are the means of three experiments.

^b Calculated logarithm of the octanol/water distribution coefficient using ChemBioDraw Ultra 14.0.

^c LE = $-1.37 \times \log(\text{IC}_{50})/N_{(\text{heavy atom})}$.

^d LLE = $-\log(\text{IC}_{50}) - \text{cLogP}$.

^e n. d.: not determined.

potential genotoxicity of aromatic amines, the amino group in **3** was derivatized into dimethylamino (**4**) and different ureido groups (**5**, **6**, **7**, and **8**), which resulted in a significant drop in potency, but most of them are more potent than **2**. These data suggest that amine derivatives have potential benefits for improving activity. On the right-hand side, structure modifications of carboxyisopropanyl moiety in GFT505 were also relatively tolerated. For example, the prolonged-carbon-chain acid **11** and **13**, amide analog **14** and installation of water-soluble morpholine **15** showed slightly increased activities on inhibiting NLRP3-mediated IL-1 β release. Removal of two branched methyl groups or insertion of vinylidene group did not improve the potency. Notably, when carboxyisopropanyl was replaced with a hydroxyethoxyl moiety as in **10**, the inhibitory potency was improved by 3-fold as compared to GFT505. These data seem to indicate that a suitable hydrogen bonding at C-4 position is potentially beneficial to inhibitory activity.

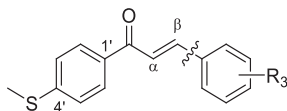
During optimization of GFT505, our synthetic compound quality was monitored by analyzing two metrics, ligand efficiency (LE) and

ligand lipophilicity efficiency (LLE) values: LE is an assessment of the efficiency of potency per heavy atom in a ligand or measuring the potency regarding ligand size, while LLE refers to an approximate measure of the balance between potency and lipophilicity [34–37]. Therefore, the LE and LLE values were valuable guides for our hit optimization which aimed to increase potency while reducing MW and lipophilicity (cLogP). In the evolution of GFT505 to **10**, the LE and LLE values were improved from 0.22 to 0.28 and from -0.71 to 0.57, respectively.

Next, we chose to maintain the C-1 vinyl ketone group of GFT505 while studying the SAR of aromatic substituent at β position on the inhibitor core (Table 2). A ring-fused ester of **10** formed compound **16**, which hindered the hydrogen bonding of the original alcohol as a hydrogen bond donor, resulting in a 2-fold potency loss (IC₅₀ = 24.2 μ M) as compared to **10** (Table 2). As intended, removing carboxyisopropanyl moiety to expose the OH group of phenol (**17**) significantly improved the inhibitory potency to 2.1 μ M, a >18-fold increase as compared to that of GFT505. The quality metrics, LE and LLE, was increased to 0.37 and 1.16. An addition of

Table 2

Inhibitory potency of analogues 16–29 on IL-1 β release mediated by NLRP3 inflammasome activation in J774A.1 Cells.



Compd	R ₃	IC ₅₀ (μ M) ^d	cLogP ^b	LE ^c	LLE ^d
16		24.2 \pm 2.3	4.19	0.30	0.43
17		2.1 \pm 0.6	4.52	0.37	1.16
18		3.5 \pm 0.2	4.03	0.36	1.43
19		14.6 \pm 0.4	3.62	0.35	1.22
20		8.8 \pm 1.0	4.07	0.35	0.99
21		10.0 \pm 1.4	3.47	0.33	1.53
22		10.7 \pm 0.8	3.86	0.34	1.11
23		12.7 \pm 0.23	4.06	0.34	0.84
24		9.7 \pm 0.1	4.30	0.34	0.72
25		5.3 \pm 1.8	4.57	0.34	0.71
26		>40.0	4.62	n.d. ^e	n.d. ^e
27		>40.0	3.25	n.d. ^e	n.d. ^e
28		11.7 \pm 1.1	5.57	0.29	-0.64
29		1.6 \pm 0.3	3.02	0.40	2.77

^a IC₅₀ values are the means of three experiments.

^b Calculated logarithm of the octanol/water distribution coefficient using ChemBioDraw Ultra 14.0.

^c LE = $-1.37 \times \log(\text{IC}_{50})/N_{(\text{heavy atom})}$.

^d LLE = $-\log(\text{IC}_{50}) - \text{cLogP}$.

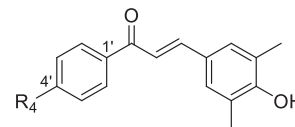
^e n. d.: not determined.

another phenolic hydroxyl (**29**: IC₅₀ = 1.6 μ M) further led to a slight improvement in IL-1 β inhibition. The importance of hydrogen bond donor is further supported by the activity results of **18** (IC₅₀ = 3.4 μ M) as a 4-CO₂H substitution with comparable inhibitory potency. Relative to other inhibitors, removal (**19**, **20**) or substitution (**21–24**, **27**, **28**) or a positional change (**25**, **26**) of two methyl groups did not improve the inhibitory potency on IL-1 β release in J774A.1 cells. Among the compounds, **29** is the most potent inhibitor against NLRP3 inflammasome activation, but it suffers from poor solubility. Taken together, compound **17** was selected for further modification based on the increase of potency, LE, and LLE.

Finally, we decided to modify the substituent at 4' position in **17** to further improve the drug-like properties. In this position, an appropriate lipophilic group was critical for inhibitory activity (Table 3). When we replaced the methylthio group with different

Table 3

Inhibitory potency of analogues 30–40 on IL-1 β release mediated by NLRP3 inflammasome activation in J774A.1 Cells.



Compd	R ₄	IC ₅₀ (μ M) ^d	cLogP ^b	LE ^c	LLE ^d
30	F	12.3 \pm 0.4	4.07	0.34	0.84
31	Cl	3.9 \pm 0.3	4.64	0.37	0.77
32	I	28.6 \pm 6.0	5.05	0.31	-0.51
33		10.6 \pm 0.3	2.69	0.31	2.28
34		12.9 \pm 0.2	2.63	0.29	2.26
35		29.4 \pm 2.9	5.74	0.25	-1.21
36		>40.0	5.63	n.d. ^e	n.d. ^e
37		>40.0	6.12	n.d. ^e	n.d. ^e
38		5.0 \pm 0.1	4.90	0.24	0.40
39		3.4 \pm 0.1	3.88	0.28	1.59
40		1.3 \pm 0.1	3.60	0.34	2.29

^a IC₅₀ values are the means of three experiments.

^b Calculated logarithm of the octanol/water distribution coefficient using ChemBioDraw Ultra 14.0.

^c LE = $-1.37 \times \log(\text{IC}_{50})/N_{(\text{heavy atom})}$.

^d LLE = $-\log(\text{IC}_{50}) - \text{cLogP}$.

^e n. d.: not determined.

halogen atoms (F, Cl, I), only chloro substitution (**31**) could maintain comparable potency against IL-1 β release. Then, methylthio group was oxidized into sulfoxides (**33**) and sulfones (**34**) to decrease cLogP values, but the inhibitory potency decreased by 5–7 fold. An obvious potency loss was also observed when we introduced the lipophilic groups, such as phenyl (**35**) and 2-thienyl (**36**, **37**), with the increasing the cLogP values of above 5. In contrast, substitution of hydrophilic fragments (**38**, **39**) at C-4' contributed to the recovery of inhibitory potency. The acrylamide group exists in many marketed drugs, and its incorporation can improve the drug-like properties of drug candidates [38–41]. Thus, we installed the acrylamide group at C-4', and the resulting compound **40** is the most potent one in all series of analogues with an IC₅₀ of 1.3 μ M. In addition, the cLogP value of **40**, compared with **17**, was further reduced from 4.5 to 3.6 while improving LLE value from 1.16 to 2.29, and the LE value was maintained.

2.3. Drug-likeness evaluation

To the class of compounds having a Michael acceptor, weak electrophilicity is a necessary requirement for the development of safe covalent drugs [22]. Therefore, GFT505, **2**, **17**, and **40**, containing α , β -unsaturated carbonyl structure, were tested for reactivity as Michael acceptor. Compounds were reacted with an excess amount of glutathione (GSH, 20 eq.) in phosphate buffer solution (pH = 7.4) at 37 °C using DMSO as the cosolvent. Interestingly, GFT505 showed much higher reactivity than **17** and **40** (Fig. 3). We

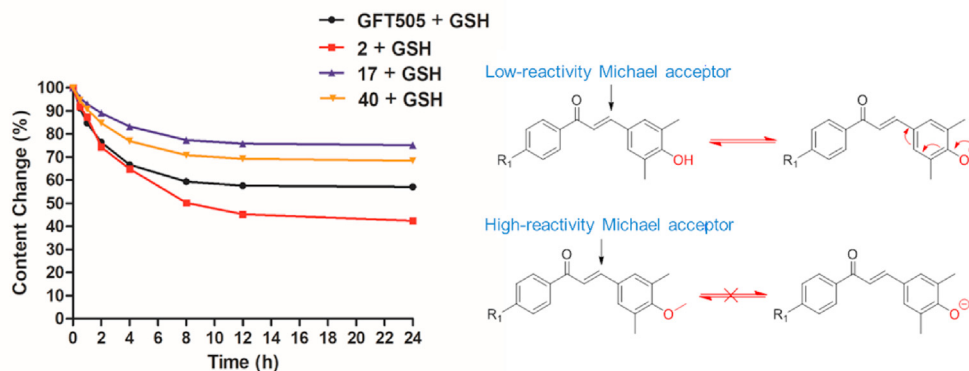


Fig. 3. Reactivity of GFT505, 2, 17 and 40 with glutathione as Michael acceptors.

proposed that a stronger electron-donating conjugation of phenolate anion in **17** and **40**, formed by deprotonation of PBS solution, resulted in significantly reduced electrophilic reactivity of α , β -unsaturated ketone with GSH. The importance of para-phenol is supported by the higher reactivity results of **2** (a methyl ether of **17**). These findings indicate **17** and **40** can be regarded as a “safe” covalent and irreversible inhibitor with weak electrophilicity. These also suggest the possible presence of specific covalent binding to biological nucleophiles and a reduced possibility of triggering hypersensitivity reactions [22].

As shown in Table 4, our lead compound **40** possessed excellent physicochemical profiles to obey Lipinski's rule of five or Veber's parameters. The safety of GFT505, **17** and **40** was evaluated with cytotoxic activities against normal human embryonic kidney 293T cell line (HEK293T). Compound **40** ($TC_{50} = 155.6 \mu\text{M}$) showed similar cytotoxicity to GFT505 ($TC_{50} = 141.5 \mu\text{M}$), but the cytotoxicity was lower than **17** ($TC_{50} = 86.2 \mu\text{M}$) toward HEK293T cells. This also suggests that the potency and cytotoxicity of **40** do not entirely depend on its Michael-acceptor reactivity toward thiols. As a result, the selectivity index [ratio of TC_{50} (HEK-293T) versus IC_{50} (J774A.1)] for **40** was high up to 119.7. These findings suggest that **40** as an NLRP3 inhibitor may be safe for normal human cells when administrated. Therefore, compound **40**, which showed potent inhibition of IL-1 β release and possessed good drug-like properties, was selected as a promising lead for further investigation.

2.4. Study on the selectivity of compound **40** to inhibit inflammasome

To confirm the effect of **40** on NLRP3 inflammasome activation, its cytotoxic activity was firstly evaluated. Compound **40** did not show any toxicity against J774A.1 cells in 2 h of incubation, and only high-concentration drug treatment showed slight cytotoxicity in 24 h of incubation (Fig. S1). Then, we treated LPS-primed J774A.1 cells and mouse bone marrow-derived macrophages

Table 4
Properties of compounds 16 and 40.

Compd	MW	HBD	HBA	cLogP ^a	tPSA	IC_{50} (μM) ^b	TC_{50} (μM) ^c	SI ^d
GFT505	384.5	1	5	5.1	63.6	39.6	141.5 \pm 7.9	3.6
17	298.4	1	3	4.5	37.3	2.1	86.2 \pm 12.8	41.0
40	321.4	2	3	3.6	66.4	1.3	155.6 \pm 9.1	119.7

^a Calculated logarithm of the octanol/water distribution coefficient using ChemBioDraw Ultra 14.0.

^b 50% inhibition concentration of IL-1 β in J774A.1 cells.

^c 50% cytotoxic concentration against HEK-293T.

^d The selectivity index (SI) is the ratio of TC_{50} (HEK-293T) versus IC_{50} (J774A.1).

(BMDMs) with **40** before nigericin stimulation. **40** produced a concentration-dependent inhibition of IL-1 β secretion by ELISA in both cell models (Fig. 4A and B). Western blot experiments showed that **40** blocked caspase-1 p20 maturation and IL-1 β secretion in a dose-dependent manner, but did not affect pro-IL-1 β , pro-caspase-1, NLRP3, or ASC in cell lysates (Fig. 4C). This suggests **40** acts in the NLRP3 activation step rather than the priming step. The lactate dehydrogenase (LDH) activity, used as a marker of cell pyroptosis, was measured in the supernatant of nigericin-treated J774A.1 cells. Pyroptosis induced by LPS/nigericin was significantly prevented by compound **40** (Fig. 4D). Furthermore, **40** had not inhibitory effect on AIM2 or NLRP4 inflammasome activation (Fig. 4E and F). The results demonstrate that **40** specifically inhibits NLRP3 inflammasome-dependent caspase-1 activation and IL-1 β secretion via acting in the NLRP3 activation step.

2.5. Biological mechanism study

Chalcones were thought to have various pharmacological activities via the regulation of ROS apoptotic pathway [42–44]. ROS has also shed light on NLRP3 inflammasome activation step. On the basis of the effects of chalcones on ROS, we hypothesized that compound **40** might inhibit this NLRP3 inflammasome activation through suppressing ROS production. As expected, treatment with **40** remarkably decreased the intracellular ROS generation accessed by Muse Cell Analyzer (Fig. 5A and B) and a fluorescence microplate reader (Fig. 5C). Next, we detected mitochondrial ROS (mtROS) by utilizing a more specific fluorescent probe MitoSOX Red (mitochondrial superoxide indicator). As shown in Fig. 5D and E, LPS/nigericin stimulation induced mitochondrial ROS production and IL-1 β release in J774A.1 cells. A mitochondria-targeted antioxidant Mitoquinone (MitoQ) was adopted as a positive reference drug. Obviously, MitoQ decreased mtROS generation, which could contribute to the inhibition of IL-1 β secretion. For compound **40**, our results reveal that its effect on the inhibition of NLRP3 inflammasome activation may also depend on mtROS reduction. mtROS production is closely linked to mitochondrial dysfunction, which was thought to be an important signal for NLRP3 inflammasome activation. Taken together, a direct correlation between the extent of the ROS inhibition and the activity against IL-1 β release suggests that **40** inhibits NLRP3 inflammasome activation via suppressing ROS production.

2.6. In vivo efficacy of compound **40**

To verify the potential of **40** to suppress inflammatory responses, we first investigated its effect on inhibiting the NLRP3-

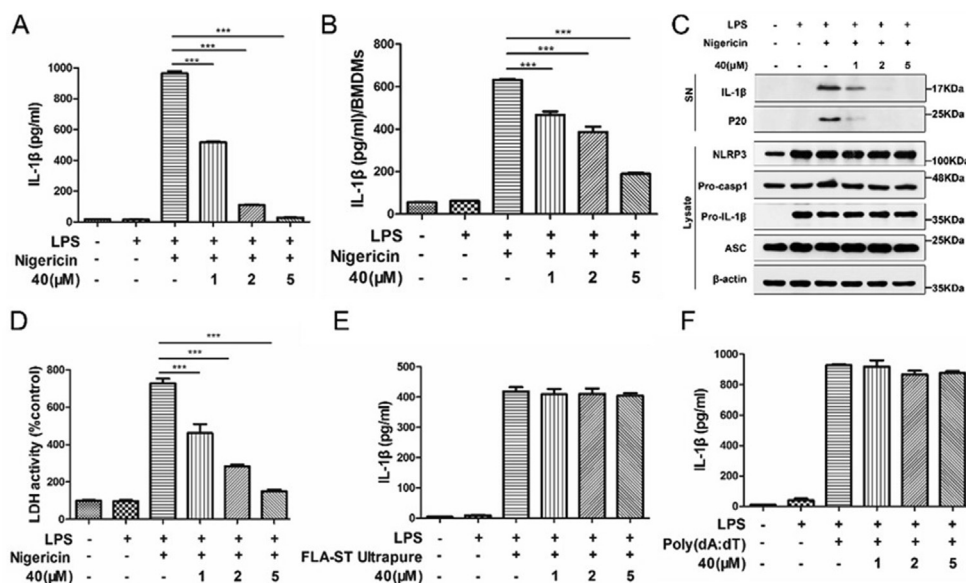


Fig. 4. Compound **40** specifically suppresses NLRP3 inflammasome activation and prevents pyroptosis *in vitro*. (A–D) LPS primed-macrophages were treated with various doses of compound **40** for 1 h and then stimulated with nigericin in J774A.1 cells (A) and BMDMs (B) for another 1 h, then cells culture supernatants were analyzed by ELISA for IL-1 β (A–B). N = 3. The value of LDH activity was normalized to that of Control. N = 5. J774A.1 cells stimulated as usual, Western blot analysis of cleaved IL-1 β , activated caspase-1 (P20) in culture supernatants (SN) and NLRP3, pro-IL-1 β , pro-caspase-1, ASC in lysates of J774A.1 cells (C). Supernatants were also analyzed by the LDH release assay for pyroptosis (D). (E, F) ELISA of IL-1 β in SN from LPS primed-J774A.1 cells treated with compound **40** for 1 h and then stimulated with FLA-ST Ultrapure (E) or poly (dA:dT) (F). N = 5. Data are represented as mean \pm SEM. One-Way ANOVA Statistics were used for statistical analysis and analyzed using an: Compared with LPS/nigericin treated group, *P < 0.05, **P < 0.01, ***P < 0.001.

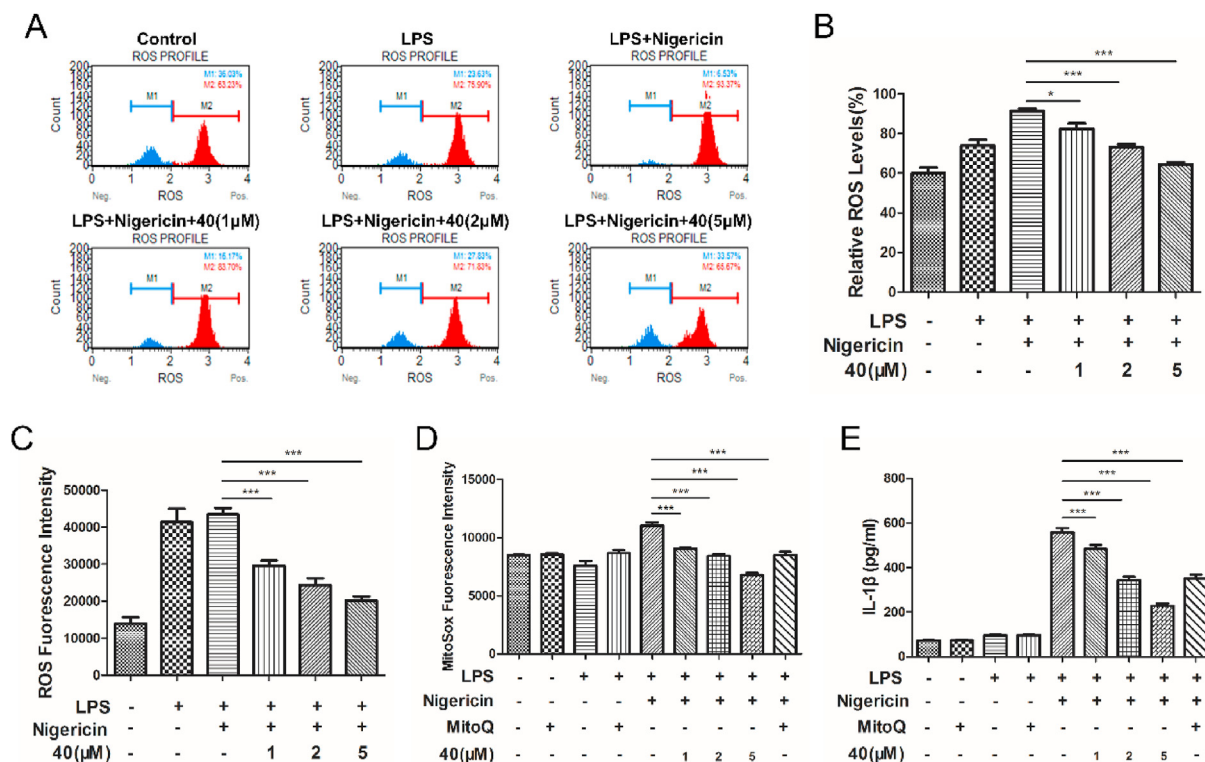


Fig. 5. Compound **40** inhibits ROS production *in vitro*. (A–C) LPS-primed J774A.1 cells were treated with various dose of compound **40** for 1 h and then stimulated with nigericin for another 1 h. Then, the cells were loaded with DHE or DCFH-DA for intracellular ROS measurement assessed by Muse Cell Analyzer (n = 3) (A, B) and a fluorescence microplate reader (n = 5) (C). (D–E) LPS primed-J774A.1 cells were treated with MitoQ or **40** (D, E) for 1 h and stimulated with nigericin for another 1 h, and then medium supernatants were analyzed by ELISA for IL-1 β (D) and the cells were stained with MitoSOX Red (5 μ M) for mtROS measurement analyzed by a fluorescence microplate reader (n = 5) (E). Compared with LPS/nigericin treated group, *P < 0.05, **P < 0.01, ***P < 0.001.

driven inflammation in mice models of LPS-induced sepsis [20]. As shown in Fig. 6, mice were injected intraperitoneally with LPS and

showed significantly increased IL-1 β level in lavage fluid. Our results showed that oral administration of **40** obviously reduced the

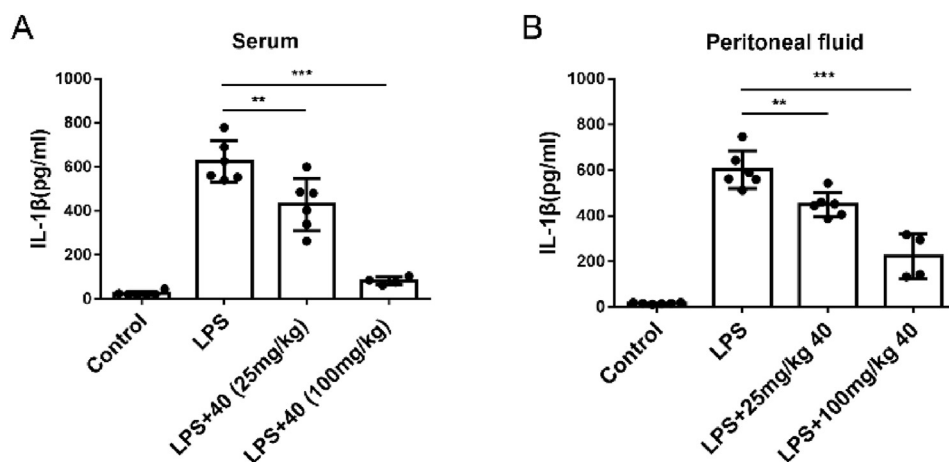


Fig. 6. Compound **40** alleviates peritoneal inflammation in sepsis. (A and B) ELISA of IL-1β in the serum (A) or peritoneal cavity (B) of C57BL/6 mice intraperitoneally injected with LPS (20 mg/kg) with or without compound **40** (25 mg/kg or 100 mg/kg). Data are representative of n = 4–6 and are means ± SEM. Compared with LPS treated group, *P < 0.05, **P < 0.01, ***P < 0.001.

level of IL-1β in both serum and peritoneal fluid in a dose-dependent manner. Thus, these results suggest that the inhibitor **40** effectively prevents acute inflammation in vivo in sepsis.

Next, we tested the therapeutic potential of **40** in vivo using a model of dextran sodium sulfate (DSS)-induced ulcerative colitis [45,46]. Seven days after being fed with 2% DSS-containing drinking water, the inflamed mice were characterized by a shortened colonic length (Fig. 7A and B) caused by fecal occlumency and increasing severity of fecal occult blood (Fig. 7C and D) and inflammation

(Fig. 7E) as compared to the control group. Intra-gastric administration of inhibitor **40** (25 and 100 mg/kg) significantly dose-dependently attenuated the decrease in colon length and fecal occult blood. In particular, IL-1β levels in colonic tissue, associated with the induction of colitis, were assessed by ELISA assays. Our results showed that treatments with **40** significantly prevented the increments of colonic IL-1β levels as compared to the control group.

Taken together, our findings show that **40** can exert beneficial effects on inflammatory diseases including sepsis and colitis by

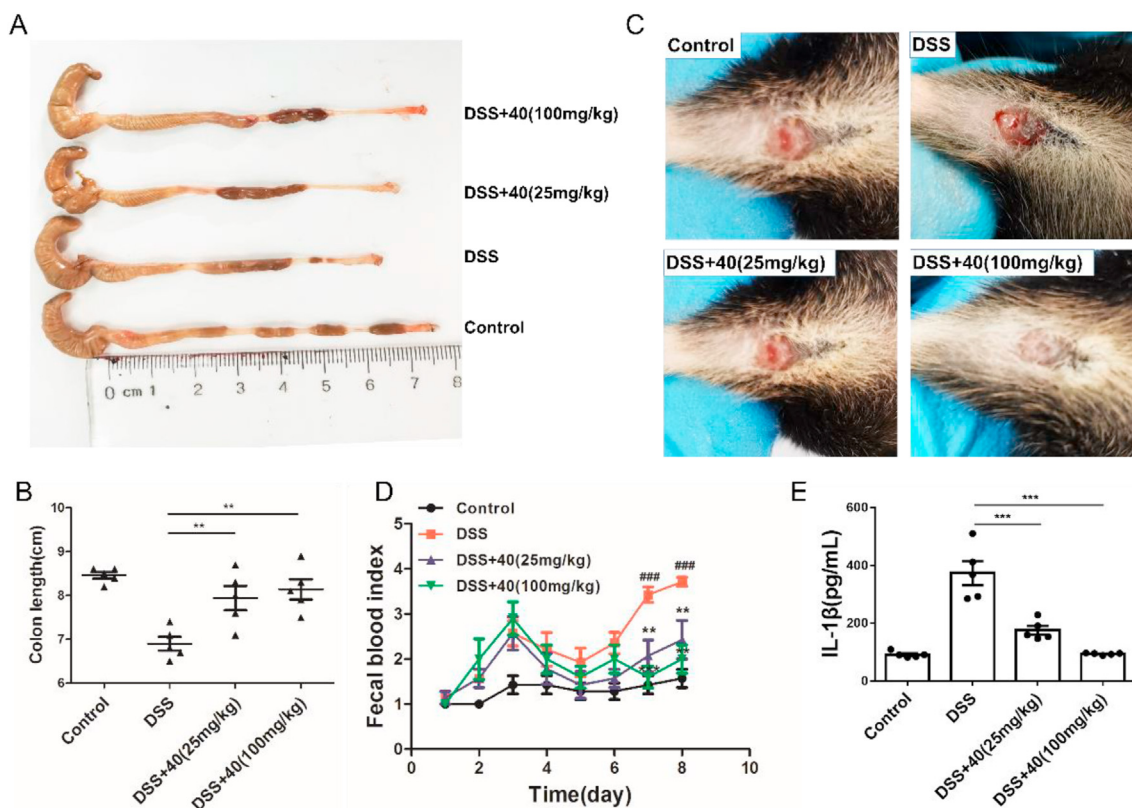


Fig. 7. Compound **40** ameliorates DSS-induced ulcerative colitis in mice. (A) The colon was photographed. (B) The length of the colon was measured when the mice were sacrificed. (C and D) Feces were collected from mice per day, and blood content was tested in fecal occult blood. (E) Protein levels of IL-1β in colon homogenates were examined by ELISA. N = 5–7. Data are represented as mean and SEM. Compared with Control group, ###P < 0.01, ####P < 0.001; Compared with DSS treated group, **P < 0.01, ***P < 0.001.

reducing the level of pro-inflammatory cytokine IL-1 β mediated by NLRP3 activation. Thus, these suggest that the blockade of NLRP3 activation could represent a promising drug target for inflammation and its related disease.

3. Conclusions

A clinical compound library screen was used to identify a novel NLRP3-inflammasome inhibitor elafibranor (GFT505), which was clinically proved to possess good safety. Starting from the low potency and low LLE hit, we optimized the chalcone pharmacophore by utilizing both simplification and replacement strategies guided by SAR and structure information. A tentative SAR study demonstrated that a suitable hydrogen bond donor at C-4 position is conducive to inhibitory activity. A breakthrough came from the removal of carboxyisopropanyl moiety with releasing the hydrogen bonding of phenol, which effectively propelled the potency into the low micromolar level. Further SAR study revealed the 3, 5-dimethyl in phenol moiety are essential to the potency on inhibiting NLRP3 inflammasome activation as positional change or removal of them led to a decrease of inhibitory activity. Then, structural modifications on the methylthio moiety led to a new lead compound **40**, which is approximately 30 times more potent against NLRP-3 inflammasome activation and lower toxicity than that of GFT505 at the cellular level. Indeed, **40** is a preferable lead of good drug-like properties, such as lower MW and lipophilicity (cLogP), higher LE and LLE. Further mechanistical characterization indicate the inhibitory potency of **40** against the NLRP3 inflammasome activation via suppressing ROS production. The in vivo ability of **40** to alleviate sepsis and colitis after oral administration was confirmed. Moreover, **40**, used as a chemical probe, is undergoing chemoproteomic studies to identify its cellular binding target, which will direct further pharmacological investigation. Collectively, the results strongly support further chemical development of **40** as a promising lead for NLRP3 inhibitors and explore their therapeutic potential for inflammation and related diseases.

4. Experimental

4.1. Chemistry

4.1.1. General

Unless otherwise mentioned, all reactions were carried out under a nitrogen atmosphere with anhydrous solvents from commercial sources (Alfa, Innochem, and Shanghai Chemical Reagent Company) without further purification. Yields refer to chromatographically homogeneous materials, unless otherwise stated. Reactions were monitored by thin-layer chromatography carried out on 0.25 mm Yantai silica gel plates (60F-254). Visualization was achieved using UV light, or phosphomolybdic acid in ethanol followed by heating. Tsingdao silica gel (200–300 mesh) was used for flash column chromatography. NMR spectra were recorded with a 400 MHz (¹H NMR, 400 MHz; ¹³C NMR, 100 MHz) spectrometer. Data are reported as follows: chemical shift, multiplicity (s = singlet, d = doublet, t = triplet, q = quartet, br = broad, m = multiplet), coupling constants, and integration.

4.1.2. General produce a for the preparation of 2–4, 16

To a solution of **1a–c** (1.0 equiv.) and **2a** or **2c** (1.0 equiv.) in methanol was added sodium hydroxide (10.0 equiv.). The solution was stirred at room temperature for 24 h. The forming precipitate was filtered and recrystallized in methanol to give title compounds **2–4**.

(E)-1-(4-methoxy-3,5-dimethylphenyl)-1-(4-(methylthio)phenyl)prop-2-en-1-one (2). Compound **2** was prepared from 4-

methylthioacetophenone **1a** (200 mg, 1.20 mmol) and 3,5-Dimethyl-4-methoxybenzaldehyde **2a** (197 mg, 1.20 mmol) according to the general synthetic procedure A as a white solid (290 mg, yield 77%). ¹H NMR (400 MHz, CDCl₃) δ 7.97–7.93 (m, 2H), 7.72 (d, *J* = 15.6 Hz, 1H), 7.42 (d, *J* = 15.6 Hz, 1H), 7.33–7.27 (m, 2H), 3.75 (s, 3H), 2.53 (s, 3H), 2.32 (s, 6H); ¹³C NMR (100 MHz, CDCl₃) δ 189.4, 159.4, 145.6, 144.6, 134.8, 131.7, 130.6, 129.4, 129.1, 125.2, 120.7, 59.9, 16.4, 15.0; HRMS (ESI) calcd for C₁₉H₂₀O₂S (M + H)⁺ 313.1257, found 313.1278.

(E)-1-(4-aminophenyl)-3-(4-methoxy-3,5-dimethylphenyl)prop-2-en-1-one (3). Compound **3** was prepared from 4-aminoacetophenone **1b** (1.00 g, 7.40 mmol) and **2a** (1.22 g, 7.40 mmol) according to the general synthetic procedure A as a yellow solid (1.30 g, yield 62%). ¹H NMR (400 MHz, DMSO-*d*₆) δ 7.97–7.87 (m, 2H), 7.75 (d, *J* = 15.4 Hz, 1H), 7.57–7.42 (m, 3H), 6.69–6.56 (m, 2H), 6.15 (s, 2H), 3.68 (s, 3H), 2.25 (s, 3H); ¹³C NMR (100 MHz, DMSO-*d*₆) δ 185.8, 158.3, 153.8, 141.3, 131.1, 130.9, 130.6, 129.2, 125.5, 121.1, 112.7, 59.4, 15.9; HRMS (ESI) calcd for C₁₈H₁₉NO₂ (M + H)⁺ 282.1489, 282.1489.

(E)-1-(4-(dimethylamino)phenyl)-3-(4-methoxy-3,5-dimethylphenyl)prop-2-en-1-one (4) Compound **4** was prepared from 4-dimethylaminoacetophenone **1c** (126 mg, 0.77 mmol) and **2a** (126 mg, 0.77 mmol) according to the general synthetic procedure A as a yellow solid (177 mg, yield 75%). ¹H NMR (400 MHz, DMSO-*d*₆) δ 8.14–8.00 (m, 2H), 7.78 (d, *J* = 15.5 Hz, 1H), 7.59–7.51 (m, 3H), 6.80–6.70 (m, 2H), 3.68 (s, 3H), 3.04 (s, 6H), 2.26 (s, 6H); ¹³C NMR (100 MHz, DMSO-*d*₆) δ 186.1, 158.4, 153.3, 141.5, 130.9, 130.7, 130.6, 129.2, 125.3, 121.1, 110.8, 59.4, 39.6, 15.8; HRMS (ESI) calcd for C₂₀H₂₃NO₂ (M + H)⁺ 310.1802, found 310.1804.41.

(E)-3-(2,3-dihydrobenzofuran-5-yl)-1-(4-(methylthio)phenyl)prop-2-en-1-one (16). Compound **16** was prepared from **1a** (90 mg, 0.54 mmol) and 2,3-dihydrobenzofuran-5-carbaldehyde **2c** (80 mg, 0.54 mmol) according to the general synthetic procedure A as a yellow solid (118 mg, yield 74%). ¹H NMR (400 MHz, DMSO-*d*₆) δ 8.12–8.05 (m, 2H), 7.85 (d, *J* = 1.7 Hz, 1H), 7.77 (d, *J* = 15.4 Hz, 1H), 7.69 (d, *J* = 15.4 Hz, 1H), 7.61 (dd, *J* = 8.3, 1.9 Hz, 1H), 7.42–7.36 (m, 2H), 6.84 (d, *J* = 8.3 Hz, 1H), 4.61 (t, *J* = 8.7 Hz, 2H), 3.23 (t, *J* = 8.7 Hz, 2H), 2.55 (s, 3H); ¹³C NMR (100 MHz, DMSO-*d*₆) δ 187.7, 162.2, 145.2, 144.2, 134.1, 130.7, 128.9, 128.6, 127.5, 125.4, 124.9, 118.6, 109.3, 71.8, 28.6, 14.0; HRMS (ESI) calcd for C₁₈H₁₆O₂S (M + H)⁺ 297.0944, found 297.0967.

4.1.3. General produce B for the preparation of 5–8

To a solution of **3** (1.0 equiv.) in toluene (1.5 mL) was added corresponding isocyanate (2.0 equiv.). The mixture was stirred at 70 °C overnight. The forming precipitate was filtered, washed with toluene and dried to obtain target compounds.

(E)-1-isopropyl-3-(4-(3-(4-methoxy-3,5-dimethylphenyl)acryloyl)phenyl)urea (5). Compound **5** was prepared from **3** (50 mg, 0.18 mmol) and isopropyl isocyanate (30 mg, 0.36 mmol) according to the general synthetic procedure B as a yellow solid (48 mg, yield 74%). ¹H NMR (400 MHz, DMSO-*d*₆) δ 8.78 (s, 1H), 8.10–8.03 (m, 2H), 7.80 (d, *J* = 15.5 Hz, 1H), 7.63–7.52 (m, 5H), 6.19 (d, *J* = 7.5 Hz, 1H), 3.84–3.74 (m, 1H), 3.69 (s, 3H), 2.26 (s, 6H), 1.11 (d, *J* = 6.5 Hz, 6H); ¹³C NMR (100 MHz, DMSO-*d*₆) δ 187.1, 158.7, 154.0, 145.3, 142.7, 131.0, 130.4, 130.3, 130.1, 129.5, 120.8, 116.6, 59.4, 41.1, 22.9, 15.9; HRMS (ESI) calcd for C₂₂H₂₆N₂O₃ (M + H)⁺ 367.2016, found 367.2013.

(E)-1-(4-(3-(4-methoxy-3,5-dimethylphenyl)acryloyl)phenyl)-3-propylurea (6). Compound **6** was prepared from **3** (50 mg, 0.18 mmol) and propyl isocyanate (30 mg, 0.36 mmol) according to the general synthetic procedure B as a yellow solid (49 mg, yield 74%). ¹H NMR (400 MHz, DMSO-*d*₆) δ 8.91 (s, 1H), 8.11–8.00 (m, 2H), 7.80 (d, *J* = 15.5 Hz, 1H), 7.69–7.49 (m, 5H), 6.33 (t, *J* = 5.7 Hz, 1H), 3.69 (s, 3H), 3.11–3.02 (m, 2H), 2.26 (s, 6H),

1.54–1.39 (m, 2H), 0.88 (t, $J = 7.4$ Hz, 3H); ^{13}C NMR (100 MHz, DMSO- d_6) δ 187.1, 158.7, 154.8, 145.4, 142.7, 131.0, 130.4, 130.4, 129.5, 120.8, 116.6, 59.4, 40.9, 22.9, 15.9, 11.4; HRMS (ESI) calcd for $\text{C}_{22}\text{H}_{26}\text{N}_2\text{O}_3$ ($\text{M} + \text{H}$) $^+$ 367.2016, found 367.2019.

(E)-1-(4-fluorophenyl)-3-(4-(3-(4-methoxy-3,5-dimethylphenyl)acryloyl)phenyl)urea (7). Compound **7** was prepared from **3** (50 mg, 0.18 mmol) and 4-fluorophenyl isocyanate (48 mg, 0.36 mmol) according to the general synthetic procedure B as a yellow solid (70 mg, 94%). ^1H NMR (400 MHz, DMSO- d_6) δ 9.14 (s, 1H), 8.85 (s, 1H), 8.18–8.04 (m, 2H), 7.82 (d, $J = 15.5$ Hz, 1H), 7.67–7.55 (m, 5H), 7.53–7.44 (m, 2H), 7.21–7.08 (m, 2H), 3.69 (s, 3H), 2.26 (s, 6H); ^{13}C NMR (100 MHz, DMSO- d_6) δ 187.2, 158.7, 157.6 (d, $J = 237.0$ Hz), 152.3, 144.4, 142.9, 135.6 (d, $J = 2.6$ Hz), 131.2, 130.9, 130.3, 130.0, 129.5, 120.3 (d, $J = 7.9$ Hz), 120.3, 117.3, 115.4 (d, $J = 22.3$ Hz) 59.4, 15.8; HRMS (ESI) calcd for $\text{C}_{25}\text{H}_{23}\text{FN}_2\text{O}_3$ ($\text{M} + \text{H}$) $^+$ 419.1765, found 419.1777.

(E)-1-(4-(3-(4-methoxy-3,5-dimethylphenyl)acryloyl)phenyl)-3-(p-tolyl)urea (8). Compound **8** was prepared from **3** (50 mg, 0.18 mmol) and 4-tolyl isocyanate (47 mg, 0.36 mmol) according to the general synthetic procedure B as a yellow solid (66 mg, yield 89%). ^1H NMR (400 MHz, DMSO- d_6) δ 9.10 (s, 1H), 8.70 (s, 1H), 8.18–8.01 (m, 2H), 7.82 (d, $J = 15.4$ Hz, 1H), 7.67–7.50 (m, 5H), 7.41–7.28 (m, 2H), 7.16–7.02 (m, 2H), 3.69 (s, 3H), 2.27 (s, 6H), 2.25 (s, 3H); ^{13}C NMR (100 MHz, DMSO- d_6) δ 187.2, 158.7, 152.2, 144.5, 142.9, 136.7, 131.1, 131.1, 130.9, 130.3, 130.0, 129.5, 129.2, 120.7, 118.6, 117.2, 59.4, 20.4, 15.8; HRMS (ESI) calcd for $\text{C}_{26}\text{H}_{26}\text{N}_2\text{O}_3$ ($\text{M} + \text{H}$) $^+$ 415.2016, found 415.2021.

4.1.4. General procedure C for the preparation of **17**, **19–32**, **35–40**

To a solution of 4 M HCl in methanol were added **1a** or **1d–1** (1.0 equiv.) and **2b** or **2e–o** (1.0 equiv.). The solution was stirred at room temperature for 24 h. The forming precipitate was filtered and dried to obtain target compounds.

(E)-3-(4-hydroxy-3,5-dimethylphenyl)-1-(4-(methylthio)phenyl)prop-2-en-1-one (17). Compound **17** was prepared from 4-methylthioacetophenone **1a** (2.33 g, 14.00 mmol) and 3,5-dimethyl-4-hydroxybenzaldehyde **2b** (2.10 g, 14.00 mmol) according to the general synthetic procedure C as a yellow solid (3.20 g, yield 77%). ^1H NMR (400 MHz, DMSO- d_6) δ 8.94 (s, 1H), 8.14–8.02 (m, 2H), 7.71 (d, $J = 15.4$ Hz, 1H), 7.60 (d, $J = 15.4$ Hz, 1H), 7.49 (s, 2H), 7.43–7.34 (m, 2H), 2.55 (s, 3H), 2.20 (s, 6H); ^{13}C NMR (100 MHz, DMSO- d_6) δ 187.8, 156.3, 145.2, 144.6, 134.2, 129.7, 129.0, 125.8, 125.0, 124.7, 118.2, 16.7, 14.0; HRMS (ESI) calcd for $\text{C}_{18}\text{H}_{18}\text{O}_2\text{S}$ ($\text{M} + \text{H}$) $^+$ 299.1100, found 299.1106.

(E)-3-(4-hydroxyphenyl)-1-(4-(methylthio)phenyl)prop-2-en-1-one (19). Compound **19** was prepared from **1a** (680 mg, 4.09 mmol) and 4-hydroxybenzaldehyde **2e** (500 mg, 4.09 mmol) according to the general synthetic procedure C as a yellow solid (667 mg, yield 60%). ^1H NMR (400 MHz, DMSO- d_6) δ 10.11 (s, 1H), 8.10–8.03 (m, 2H), 7.76–7.64 (m, 4H), 7.43–7.32 (m, 2H), 6.88–6.80 (m, 2H), 2.55 (s, 3H); ^{13}C NMR (100 MHz, DMSO- d_6) δ 187.8, 160.1, 145.1, 144.2, 134.1, 131.0, 128.9, 125.9, 124.9, 118.3, 115.9, 14.0; HRMS (ESI) calcd for $\text{C}_{16}\text{H}_{14}\text{O}_2\text{S}$ ($\text{M} + \text{H}$) $^+$ 271.0787, found 271.0812.

(E)-3-(4-hydroxy-3-methylphenyl)-1-(4-(methylthio)phenyl)prop-2-en-1-one (20). Compound **20** was prepared from **1a** (300 mg, 1.80 mmol) and 4-hydroxy-3-methylbenzaldehyde **2f** (245 mg, 1.80 mmol) according to the general synthetic procedure C as a yellow solid (325 mg, yield 63%). ^1H NMR (400 MHz, DMSO- d_6) δ 10.00 (s, 1H), 8.12–7.99 (m, 2H), 7.73–7.66 (m, 2H), 7.63 (d, $J = 15.4$ Hz, 1H), 7.51 (dd, $J = 8.3, 2.2$ Hz, 1H), 7.41–7.35 (m, 2H), 6.85 (d, $J = 8.3$ Hz, 1H), 2.55 (s, 3H), 2.17 (s, 3H); ^{13}C NMR (100 MHz, DMSO- d_6) δ 187.7, 158.4, 145.0, 144.4, 134.2, 131.3, 128.9, 125.7, 124.9, 124.7, 118.0, 114.9, 15.9, 14.0; HRMS (ESI) calcd for $\text{C}_{17}\text{H}_{16}\text{O}_2\text{S}$ ($\text{M} + \text{H}$) $^+$ 285.0944, found 285.0968.

(E)-3-(4-hydroxy-3-methoxyphenyl)-1-(4-(methylthio)

phenyl)prop-2-en-1-one (21). Compound **21** was prepared from **1a** (300 mg, 1.80 mmol) and 4-hydroxy-3-methoxybenzaldehyde **2g** (274 mg, 1.80 mmol) according to the general synthetic procedure C as a yellow solid (275 mg, yield 51%). ^1H NMR (400 MHz, DMSO- d_6) δ 9.68 (s, 1H), 8.11–8.02 (m, 2H), 7.75 (d, $J = 15.4$ Hz, 1H), 7.67 (d, $J = 15.4$ Hz, 1H), 7.51 (d, $J = 2.0$ Hz, 1H), 7.43–7.35 (m, 2H), 7.28 (dd, $J = 8.3, 1.9$ Hz, 1H), 6.84 (d, $J = 8.1$ Hz, 1H), 3.87 (s, 3H), 2.55 (s, 3H); ^{13}C NMR (100 MHz, DMSO- d_6) δ 187.8, 149.7, 148.0, 145.1, 144.6, 134.2, 128.9, 126.3, 124.9, 124.1, 118.5, 115.6, 111.7, 55.8, 14.0; HRMS (ESI) calcd for $\text{C}_{17}\text{H}_{16}\text{O}_3\text{S}$ ($\text{M} + \text{H}$) $^+$ 301.0893, found 301.0911.

(E)-3-(3-fluoro-4-hydroxyphenyl)-1-(4-(methylthio)phenyl)prop-2-en-1-one (22). Compound **22** was prepared from **1a** (300 mg, 1.80 mmol) and 3-fluoro-4-hydroxybenzaldehyde **2h** (252 mg, 1.80 mmol) according to the general synthetic procedure C as a yellow solid (155 mg, yield 30%). ^1H NMR (400 MHz, DMSO- d_6) δ 10.51 (s, 1H), 8.12–8.03 (m, 2H), 7.85 (dd, $J = 12.6, 2.1$ Hz, 1H), 7.79 (d, $J = 15.5$ Hz, 1H), 7.64 (d, $J = 15.5$ Hz, 1H), 7.52–7.47 (m, 1H), 7.41–7.36 (m, 2H), 7.06–6.88 (m, 1H), 2.55 (s, 3H); ^{13}C NMR (100 MHz, DMSO- d_6) δ 187.7, 151.2 (d, $J = 241.6$ Hz), 147.5 (d, $J = 12.5$ Hz), 145.3, 143.0 (d, $J = 2.5$ Hz), 133.9, 129.0, 126.9 (d, $J = 2.6$ Hz), 126.7 (d, $J = 6.6$ Hz), 124.9, 120.0, 117.8 (d, $J = 3.3$ Hz), 115.8 (d, $J = 18.6$ Hz), 14.0; HRMS (ESI) calcd for $\text{C}_{16}\text{H}_{13}\text{FO}_2\text{S}$ ($\text{M} + \text{H}$) $^+$ 289.0693, found 289.0712.

(E)-3-(2-fluoro-4-hydroxyphenyl)-1-(4-(methylthio)phenyl)prop-2-en-1-one (23). Compound **23** was prepared from **1a** (300 mg, 1.80 mmol) and 2-fluoro-4-hydroxybenzaldehyde **2i** (252 mg, 1.80 mmol) according to the general synthetic procedure C as a yellow solid (96 mg, yield 18%). ^1H NMR (400 MHz, DMSO- d_6) δ 10.58 (s, 1H), 8.09–8.01 (m, 2H), 7.94 (t, $J = 8.8$ Hz, 1H), 7.81–7.70 (m, 2H), 7.43–7.35 (m, 2H), 6.72 (dd, $J = 8.6, 2.3$ Hz, 1H), 6.66 (dd, $J = 12.6, 2.3$ Hz, 1H), 2.55 (s, 3H); ^{13}C NMR (100 MHz, DMSO- d_6) δ 187.7, 162.2 (d, $J = 250.0$ Hz), 161.7 (d, $J = 12.6$ Hz), 145.4, 135.5 (d, $J = 3.7$ Hz), 133.9, 130.3 (d, $J = 4.5$ Hz), 128.9, 125.0, 120.1 (d, $J = 4.3$ Hz), 113.4 (d, $J = 11.5$ Hz), 112.64 (d, $J = 2.3$ Hz), 102.9 (d, $J = 24.1$ Hz), 14.0; HRMS (ESI) calcd for $\text{C}_{16}\text{H}_{13}\text{FO}_2\text{S}$ ($\text{M} + \text{H}$) $^+$ 289.0693, found 289.0708.

(E)-3-(3-chloro-4-hydroxyphenyl)-1-(4-(methylthio)phenyl)prop-2-en-1-one (24). Compound **24** was prepared from **1a** (300 mg, 1.80 mmol) and 3-chloro-4-hydroxybenzaldehyde **2j** (282 mg, 1.80 mmol) according to the general synthetic procedure C as a yellow solid (124 mg, yield 23%). ^1H NMR (400 MHz, DMSO- d_6) δ 10.81 (s, 1H), 8.14–8.06 (m, 2H), 8.02 (d, $J = 2.1$ Hz, 1H), 7.81 (d, $J = 15.5$ Hz, 1H), 7.67–7.60 (m, 2H), 7.41–7.36 (m, 2H), 7.02 (d, $J = 8.4$ Hz, 1H), 2.55 (s, 1H); ^{13}C NMR (100 MHz, DMSO- d_6) δ 187.7, 155.3, 145.3, 142.7, 133.9, 130.1, 129.7, 129.0, 127.2, 124.9, 120.5, 119.8, 116.7, 14.0; HRMS (ESI) calcd for $\text{C}_{16}\text{H}_{13}\text{ClO}_2\text{S}$ ($\text{M} + \text{H}$) $^+$ 305.0398, found 305.0411.

(E)-3-(4-hydroxy-2,5-dimethylphenyl)-1-(4-(methylthio)phenyl)prop-2-en-1-one (25). Compound **25** was prepared from **1a** (300 mg, 1.80 mmol) and 4-hydroxy-2,5-dimethylbenzaldehyde **2k** (271 mg, 1.80 mmol) according to the general synthetic procedure C as a yellow solid (382 mg, yield 71%). ^1H NMR (400 MHz, DMSO- d_6) δ 9.87 (s, 1H), 8.17–8.01 (m, 2H), 7.92 (d, $J = 15.3$ Hz, 1H), 7.81 (s, 1H), 7.64 (d, $J = 15.3$ Hz, 1H), 7.45–7.28 (m, 2H), 6.67 (s, 1H), 2.55 (s, 3H), 2.33 (s, 3H), 2.15 (s, 3H); ^{13}C NMR (100 MHz, DMSO- d_6) δ 187.7, 158.1, 145.0, 141.0, 137.8, 134.2, 129.5, 128.9, 124.9, 123.9, 122.4, 118.4, 116.6, 19.0, 15.5, 14.0; HRMS (ESI) calcd for $\text{C}_{18}\text{H}_{18}\text{O}_2\text{S}$ ($\text{M} + \text{H}$) $^+$ 299.1100, found 299.1114.

(E)-3-(4-hydroxy-2,6-dimethylphenyl)-1-(4-(methylthio)phenyl)prop-2-en-1-one (26). Compound **26** was prepared from **1a** (300 mg, 1.80 mmol) and 4-hydroxy-2,6-dimethylbenzaldehyde **2l** (271 mg, 1.80 mmol) according to the general synthetic procedure C as a yellow solid (256 mg, yield 48%). ^1H NMR (400 MHz, DMSO- d_6) ^1H NMR (400 MHz, DMSO- d_6) δ 9.73 (s, 1H), δ 8.02–7.95 (m, 2H), 7.85 (d, $J = 15.8$ Hz, 1H), 7.40–7.35 (m, 2H), 7.28 (d,

$J = 15.8$ Hz, 1H), 6.56 (s, 2H), 2.53 (s, 3H), 2.34 (s, 6H); ^{13}C NMR (100 MHz, DMSO- d_6) δ 188.1, 158.0, 145.4, 141.6, 139.8, 134.1, 129.0, 125.1, 124.6, 124.4, 115.8, 21.6, 14.0; HRMS (ESI) calcd for $\text{C}_{18}\text{H}_{18}\text{O}_2\text{S}$ ($\text{M} + \text{H}$) $^+$ 299.1100, found 299.1113.

(E)-3-(4-hydroxy-3,5-dimethoxyphenyl)-1-(4-(methylthio)phenyl)prop-2-en-1-one (27). Compound **27** was prepared from **1a** (300 mg, 1.80 mmol) and 4-hydroxy-3,5-dimethoxybenzaldehyde **2m** (328 mg, 1.80 mmol) according to the general synthetic procedure C as a yellow solid (265 mg, yield 45%). ^1H NMR (400 MHz, DMSO- d_6) δ 9.04 (s, 1H), 8.13–8.06 (m, 2H), 7.78 (d, $J = 15.4$ Hz, 1H), 7.67 (d, $J = 15.4$ Hz, 1H), 7.43–7.36 (m, 2H), 7.20 (s, 2H), 3.85 (s, 6H), 2.56 (s, 3H); ^{13}C NMR (100 MHz, DMSO- d_6) δ 187.8, 148.1, 145.1, 145.0, 138.7, 134.1, 129.0, 125.1, 124.9, 118.9, 106.9, 56.2, 14.0; HRMS (ESI) calcd for $\text{C}_{18}\text{H}_{18}\text{O}_4\text{S}$ ($\text{M} + \text{H}$) $^+$ 331.0999, found 331.1000.

(E)-3-(3,5-diethyl-4-hydroxyphenyl)-1-(4-(methylthio)phenyl)prop-2-en-1-one (28). Compound **28** was prepared from **1a** (100 mg, 0.60 mmol) and 3,5-diethyl-4-hydroxybenzaldehyde **2n** (107 mg, 0.60 mmol) according to the general synthetic procedure C as a yellow solid (136 mg, yield 69%). ^1H NMR (400 MHz, DMSO- d_6) δ 8.81 (s, 1H), 8.19–7.99 (m, 2H), 7.72 (d, $J = 15.4$ Hz, 1H), 7.64 (d, $J = 15.4$ Hz, 1H), 7.48 (s, 2H), 7.42–7.34 (m, 2H), 2.63 (q, $J = 7.5$ Hz, 4H), 2.55 (s, 3H), 1.17 (t, $J = 7.5$ Hz, 6H); ^{13}C NMR (100 MHz, DMSO- d_6) δ 187.7, 155.2, 145.0, 144.8, 134.2, 130.9, 128.9, 128.1, 126.1, 124.9, 118.1, 23.0, 14.4, 14.0; HRMS (ESI) calcd for $\text{C}_{20}\text{H}_{22}\text{O}_2\text{S}$ ($\text{M} + \text{H}$) $^+$ 327.1413, found 327.1429.

(E)-3-(3,4-dihydroxyphenyl)-1-(4-(methylthio)phenyl)prop-2-en-1-one (29). Compound **29** was prepared from **1a** (1.20 g, 7.24 mmol) and 3,4-dihydroxybenzaldehyde **2o** (1.00 g, 7.24 mmol) according to the general synthetic procedure C as a yellow solid (960 mg, yield 46%). ^1H NMR (400 MHz, DMSO- d_6) δ 9.61 (s, 1H), 9.25 (s, 1H), 8.14–7.93 (m, 2H), 7.66–7.53 (m, 2H), 7.43–7.34 (m, 2H), 7.26 (d, $J = 2.1$ Hz, 1H), 7.18 (dd, $J = 8.2, 2.1$ Hz, 1H), 6.81 (d, $J = 8.2$ Hz, 1H), 2.55 (s, 3H); ^{13}C NMR (100 MHz, DMSO- d_6) δ 187.8, 148.7, 145.6, 145.1, 144.7, 134.2, 128.9, 126.4, 125.0, 122.2, 118.3, 115.8, 115.6, 14.0; HRMS (ESI) calcd for $\text{C}_{16}\text{H}_{14}\text{O}_3\text{S}$ ($\text{M} + \text{H}$) $^+$ 287.0736, found 287.0740.

(E)-1-(4-fluorophenyl)-3-(4-hydroxy-3,5-dimethylphenyl)prop-2-en-1-one (30). Compound **30** was prepared from 1-(4-fluorophenyl)ethan-1-one **1d** (500 mg, 3.62 mmol) and **2b** (543 mg, 3.62 mmol) according to the general synthetic procedure C as a yellow solid (618 mg, yield 63%). ^1H NMR (400 MHz, DMSO- d_6) δ 8.94 (s, 1H), 8.29–8.09 (m, 2H), 7.71 (d, $J = 15.4$ Hz, 1H), 7.62 (d, $J = 15.4$ Hz, 1H), 7.48 (s, 2H), 7.41–7.31 (m, 2H); ^{13}C NMR (100 MHz, DMSO- d_6) δ 187.4, 164.9 (d, $J = 251.3$ Hz), 156.4, 145.1, 134.7 (d, $J = 2.9$ Hz), 131.3 (d, $J = 9.2$ Hz), 129.7, 125.7, 124.7, 118.0, 115.7 (d, $J = 21.7$ Hz), 16.6; HRMS (ESI) calcd for $\text{C}_{17}\text{H}_{15}\text{FO}_2$ ($\text{M} + \text{H}$) $^+$ 271.1129, found 271.1131.

(E)-1-(4-chlorophenyl)-3-(4-hydroxy-3,5-dimethylphenyl)prop-2-en-1-one (31). Compound **31** was prepared from 1-(4-chlorophenyl)ethan-1-one **1e** (103 mg, 0.67 mmol) and **2b** (100 mg, 0.67 mmol) according to the general synthetic procedure C as a yellow solid (128 mg, yield 67%). ^1H NMR (400 MHz, DMSO- d_6) δ 8.18–8.10 (m, 2H), 7.70 (d, $J = 15.4$ Hz, 1H), 7.65–7.58 (m, 3H), 7.49 (s, 2H), 2.21 (s, 6H); ^{13}C NMR (100 MHz, DMSO- d_6) δ 187.7, 156.5, 145.4, 137.7, 136.7, 130.3, 129.8, 128.8, 125.6, 124.7, 117.9, 16.5; HRMS (ESI) calcd for $\text{C}_{17}\text{H}_{15}\text{ClO}_2$ ($\text{M} + \text{H}$) $^+$ 287.0833, found 287.0832.

(E)-3-(4-hydroxy-3,5-dimethylphenyl)-1-(4-iodophenyl)prop-2-en-1-one (32). Compound **32** was prepared from 1-(4-iodophenyl)ethan-1-one **1f** (1.64 g, 6.66 mmol) and **2b** (1.00 g, 6.66 mmol) according to the general synthetic procedure C as a yellow solid (1.10 g, yield 44%). ^1H NMR (400 MHz, DMSO- d_6) δ 7.96–7.92 (m, 2H), 7.91–7.86 (m, 2H), 7.67 (d, $J = 15.5$ Hz, 1H), 7.61 (d, $J = 15.5$ Hz, 3H), 7.49 (s, 2H), 2.20 (s, 6H); ^{13}C NMR (100 MHz,

DMSO- d_6) δ 188.3, 156.5, 145.4, 137.7, 137.3, 130.2, 129.8, 125.7, 124.7, 117.9, 101.4, 16.6; HRMS (ESI) calcd for $\text{C}_{17}\text{H}_{15}\text{IO}_2$ ($\text{M} + \text{H}$) $^+$ 379.0189, found 379.0197.

(E)-1-([1,1'-biphenyl]-4-yl)-3-(4-hydroxy-3,5-dimethylphenyl)prop-2-en-1-one (35). Compound **35** was prepared from 1-([1,1'-biphenyl]-4-yl)ethan-1-one **1g** (131 mg, 0.67 mmol) and **2b** (100 mg, 0.67 mmol) according to the general synthetic procedure C as a yellow solid (102 mg, yield 47%). ^1H NMR (400 MHz, DMSO- d_6) δ 8.27–8.18 (m, 2H), 7.87–7.81 (m, 2H), 7.80–7.71 (m, 3H), 7.65 (d, $J = 15.5$ Hz, 1H), 7.55–7.47 (m, 4H), 7.46–7.39 (m, 1H), 2.21 (s, 6H); ^{13}C NMR (100 MHz, DMSO- d_6) δ 188.5, 156.5, 145.0, 144.3, 139.1, 136.9, 129.9, 129.3, 128.5, 127.1, 127.0, 125.8, 124.8, 118.4, 16.7; HRMS (ESI) calcd for $\text{C}_{23}\text{H}_{20}\text{O}_2$ ($\text{M} + \text{H}$) $^+$ 329.1536, found 329.1537.

(E)-3-(4-hydroxy-3,5-dimethylphenyl)-1-(4-(thiophen-2-yl)phenyl)prop-2-en-1-one (36). Compound **36** was prepared from 1-(4-(thiophen-2-yl)phenyl)ethan-1-one **1h** (100 mg, 0.49 mmol) and **2b** (74 mg, 0.49 mmol) according to the general synthetic procedure C as a yellow solid (63 mg, yield 38%). ^1H NMR (400 MHz, DMSO- d_6) δ 8.96 (s, 1H), 8.24–8.12 (m, 2H), 7.88–7.79 (m, 2H), 7.78–7.70 (m, 2H), 7.69–7.60 (m, 2H), 7.51 (s, 2H), 7.20 (dd, $J = 5.1, 3.7$ Hz, 1H), 2.22 (s, 6H); ^{13}C NMR (100 MHz, DMSO- d_6) δ 187.9, 156.4, 144.9, 142.2, 137.7, 136.7, 129.8, 129.4, 128.9, 127.5, 125.7, 125.5, 125.4, 124.7, 118.2, 16.6; HRMS (ESI) calcd for $\text{C}_{21}\text{H}_{18}\text{O}_2\text{S}$ ($\text{M} + \text{H}$) $^+$ 335.1100, found 35.1103.

(E)-3-(4-hydroxy-3,5-dimethylphenyl)-1-(4-(5-methylthiophen-2-yl)phenyl)prop-2-en-1-one (37). Compound **37** was prepared from 1-(4-(5-methylthiophen-2-yl)phenyl)ethan-1-one **1i** (100 mg, 0.46 mmol) and **2b** (69 mg, 0.46 mmol) according to the general synthetic procedure C as a yellow solid (55 mg, yield 34%). ^1H NMR (400 MHz, DMSO- d_6) δ 8.95 (s, 1H), 8.18–8.08 (m, 2H), 7.80–7.68 (m, 3H), 7.62 (d, $J = 15.4$ Hz, 1H), 7.55–7.46 (m, 3H), 6.94–6.81 (m, 1H), 2.50–2.46 (m, 3H), 2.21 (s, 6H); ^{13}C NMR (100 MHz, DMSO- d_6) δ 187.8, 156.3, 144.7, 141.2, 139.7, 138.0, 136.3, 129.7, 129.4, 127.4, 125.8, 125.5, 124.8, 124.7, 118.2, 16.6, 15.2; HRMS (ESI) calcd for $\text{C}_{22}\text{H}_{20}\text{O}_2\text{S}$ ($\text{M} + \text{H}$) $^+$ 349.1257, found 349.1261.

(E)-4-fluoro-N-(4-(3-(4-hydroxy-3,5-dimethylphenyl)acryloyl)phenyl)benzenesulfonamide (38). Compound **38** was prepared from N-(4-acetylphenyl)-4-fluorobenzenesulfonamide **1j** (100 mg, 0.42 mmol) and **2b** (63 mg, 0.42 mmol) according to the general synthetic procedure C as a yellow solid (88 mg, yield 49%). ^1H NMR (400 MHz, DMSO- d_6) δ 8.93 (s, 1H), 8.07–7.99 (m, 2H), 7.95–7.86 (m, 2H), 7.62 (d, $J = 15.4$ Hz, 1H), 7.55 (d, $J = 15.4$ Hz, 1H), 7.49–7.37 (m, 4H), 7.32–7.20 (m, 2H), 2.19 (s, 6H); ^{13}C NMR (100 MHz, DMSO- d_6) δ 187.4, 164.6 (d, $J = 252.3$ Hz), 156.3, 144.5, 141.8, 135.7 (d, $J = 2.9$ Hz), 133.4, 130.0, 129.9 (d, $J = 9.7$ Hz), 129.6, 125.8, 124.7, 118.4, 118.1, 116.8 (d, $J = 23.0$ Hz), 16.6; HRMS (ESI) calcd for $\text{C}_{23}\text{H}_{20}\text{FNO}_4\text{S}$ ($\text{M} + \text{H}$) $^+$ 426.1170, found 426.1175.

(E)-3-(4-hydroxy-3,5-dimethylphenyl)-1-(4-((propan-2-yl)sulfamoyl)amino)phenyl)prop-2-en-1-one (39). Compound **39** was prepared from N-(4-acetylphenyl) isopropyl amino-sulfonamide **1k** (50 mg, 0.20 mmol) and **2b** (29 mg, 0.20 mmol) according to the general synthetic procedure C as a yellow solid (28 mg, yield 37%). ^1H NMR (400 MHz, DMSO- d_6) δ 10.22 (s, 1H), 8.90 (s, 1H), 8.13–8.01 (m, 2H), 7.77–7.64 (m, 2H), 7.57 (d, $J = 15.4$ Hz, 1H), 7.47 (s, 2H), 7.29–7.17 (m, 2H), 3.34–3.29 (m, 1H), 2.20 (s, 6H), 0.99 (d, $J = 6.5$ Hz, 6H); ^{13}C NMR (100 MHz, DMSO- d_6) δ 187.4, 156.2, 144.1, 143.6, 131.5, 129.9, 129.6, 125.9, 124.7, 118.3, 116.5, 45.2, 23.1, 16.6; HRMS (ESI) calcd for $\text{C}_{20}\text{H}_{24}\text{N}_2\text{O}_4\text{S}$ ($\text{M} + \text{H}$) $^+$ 389.1560, found 389.1532.

(E)-N-(4-(3-(4-hydroxy-3,5-dimethylphenyl)acryloyl)phenyl)acrylamide(40). Compound **40** was prepared from N-(4-acetylphenyl)acrylamide **1l** (100 mg, 0.53 mmol) and **2b** (79 mg, 0.53 mmol) according to the general synthetic procedure C as a yellow solid (112 mg, yield 66%). ^1H NMR (400 MHz, DMSO- d_6)

δ 10.51 (s, 1H), 8.94 (s, 1H), 8.17–8.11 (m, 2H), 7.87–7.81 (m, 2H), 7.71 (d, $J = 15.4$ Hz, 1H), 7.60 (d, $J = 15.4$ Hz, 1H), 7.48 (s, 2H), 6.48 (dd, $J = 17.0, 10.0$ Hz, 1H), 6.32 (dd, $J = 17.0, 2.0$ Hz, 1H), 5.82 (dd, $J = 10.0, 2.0$ Hz, 1H), 2.20 (s, 6H); ^{13}C NMR (100 MHz, DMSO- d_6) δ 187.5, 163.7, 156.3, 144.4, 143.2, 133.1, 131.6, 129.8, 129.7, 128.0, 125.9, 124.8, 118.9, 118.3, 16.6; HRMS (ESI) calcd for $\text{C}_{20}\text{H}_{19}\text{NO}_2$ ($\text{M} + \text{H}$) $^+$ 322.1438, found 322.1437.

4.1.5. General procedure D for the preparation of **9**, **11**–**13**

Step A: Preparation of carboxylic ester. To a solution of **17** (1.0 equiv.) in anhydrous DMF were added corresponding bromo-carboxylates (3.0 equiv.) and potassium carbonate (5.0 equiv.). The solution was heated to 90 °C for 6 h, then the solution was diluted with water and extracted with ethyl acetate. The organic layers were combined, concentrated and purified by column chromatography to give the desired ester.

Step B: Hydrolysis of ester. To a solution of the above ester (1.0 equiv.) in THF/H₂O (1:1, v/v) was added LiOH (6.0 equiv.). The solution was stirred at 50 °C overnight, then the solution was adjusted to pH = 2 with hydrochloric acid (1 M) and extracted with ethyl acetate. The organic layers were combined, concentrated and purified by column chromatography to obtain target compounds.

(E)-2-(2,6-dimethyl-4-(3-(4-(methylthio)phenyl)-3-oxoprop-1-en-1-yl)phenoxy)acetic acid (9). The corresponding ester was prepared from **17** (200 mg, 0.67 mmol) and ethyl bromoacetate (336 mg, 2.01 mmol) according to step A of general synthetic procedure D as a yellow oil (183 mg, yield 71%). Compound **9** was prepared from the above ester (300 mg, 0.78 mmol) according to step B of general synthetic procedure D as a yellow solid (180 mg, yield 65%). ^1H NMR (400 MHz, DMSO- d_6) δ 8.14–8.03 (m, 2H), 7.80 (d, $J = 15.5$ Hz, 1H), 7.61 (d, $J = 15.5$ Hz, 1H), 7.56 (s, 2H), 7.43–7.29 (m, 2H), 4.43 (s, 2H), 2.55 (s, 3H), 2.27 (s, 6H); ^{13}C NMR (100 MHz, DMSO- d_6) δ 187.9, 170.2, 157.4, 145.5, 143.5, 133.9, 131.1, 130.5, 129.7, 129.1, 125.0, 120.8, 68.8, 16.1, 14.0; HRMS (ESI) calcd for $\text{C}_{20}\text{H}_{20}\text{O}_4\text{S}$ ($\text{M} + \text{H}$) $^+$ 357.1155, found 357.1159.

(E)-2-(2,6-dimethyl-4-(3-(4-(methylthio)phenyl)-3-oxoprop-1-en-1-yl)phenoxy)butanoic acid (11). The corresponding ester was prepared from **17** (200 mg, 0.67 mmol) and methyl 2-bromobutanoate (363 mg, 2.01 mmol) according to step A of general synthetic procedure D as a yellow oil (210 mg, yield 79%). Compound **11** was prepared from the above ester (200 mg, 0.50 mmol) according to step B of general synthetic procedure D as a yellow solid (120 mg, yield 62%). ^1H NMR (400 MHz, DMSO- d_6) δ 8.14–8.04 (m, 2H), 7.80 (d, $J = 15.6$ Hz, 1H), 7.61 (d, $J = 15.6$ Hz, 1H), 7.55 (s, 2H), 7.44–7.35 (m, 2H), 4.44 (t, $J = 5.9$ Hz, 1H), 2.55 (s, 3H), 2.28 (s, 6H), 1.97–1.81 (m, 2H), 0.98 (t, $J = 7.4$ Hz, 3H); ^{13}C NMR (100 MHz, DMSO- d_6) δ 187.8, 172.1, 157.0, 145.5, 143.5, 133.9, 130.8, 129.9, 129.9, 129.1, 125.0, 120.6, 81.2, 25.7, 16.9, 14.0, 9.0; HRMS (ESI) calcd for $\text{C}_{22}\text{H}_{24}\text{O}_4\text{S}$ ($\text{M} + \text{H}$) $^+$ 385.1468, found 385.1473.

(E)-2-((2,6-dimethyl-4-(3-(4-(methylthio)phenyl)-3-oxoprop-1-en-1-yl)phenoxy)methyl) acrylic acid (12). The corresponding ester was prepared from **17** (200 mg, 0.67 mmol) and methyl 2-(bromomethyl)acrylate (360 mg, 2.01 mmol) according to step A of general synthetic procedure D as a yellow oil (185 mg, yield 70%). Compound **12** was prepared from the above ester (185 mg, 0.47 mmol) according to step B of general synthetic procedure D as a yellow solid (55 mg, yield 31%). ^1H NMR (400 MHz, CDCl₃) δ 7.98–7.94 (m, 2H), 7.73 (d, $J = 15.6$ Hz, 1H), 7.42 (d, $J = 15.6$ Hz, 1H), 7.35–7.28 (m, 4H), 6.60–6.56 (m, 1H), 6.29–6.25 (m, 1H), 4.56–4.52 (m, 2H), 2.54 (s, 3H), 2.31 (s, 6H); ^{13}C NMR (100 MHz, DMSO- d_6) δ 187.9, 166.8, 157.5, 145.5, 143.6, 137.6, 133.9, 131.3, 130.4, 129.7, 129.1, 126.7, 125.0, 120.8, 70.2, 16.1, 14.0; HRMS

(ESI) calcd for $\text{C}_{22}\text{H}_{22}\text{O}_4\text{S}$ ($\text{M} + \text{H}$) $^+$ 383.1312, found 383.1315.

(E)-5-(2,6-dimethyl-4-(3-(4-(methylthio)phenyl)-3-oxoprop-1-en-1-yl)phenoxy)pentanoic acid (13). The corresponding ester was prepared from **17** (200 mg, 0.67 mmol) and ethyl 5-bromopentanoate (420 mg, 2.01 mmol) according to step A of general synthetic procedure D as a yellow oil (240 mg, 84%). Compound **13** was prepared from the above ester (180 mg, 0.42 mmol) according to step B of general synthetic procedure D as a yellow solid (121 mg, yield 72%). ^1H NMR (400 MHz, DMSO- d_6) δ 8.12–8.06 (m, 2H), 7.80 (d, $J = 15.5$ Hz, 1H), 7.62 (d, $J = 15.5$ Hz, 1H), 7.57 (s, 2H), 7.43–7.36 (m, 2H), 3.77 (t, $J = 5.8$ Hz, 2H), 2.56 (s, 3H), 2.31 (t, $J = 6.9$ Hz, 2H), 2.25 (s, 6H), 1.77–1.70 (m, 4H); ^{13}C NMR (100 MHz, DMSO- d_6) δ 187.8, 174.5, 157.9, 145.4, 143.6, 133.9, 131.1, 130.1, 129.6, 129.0, 124.9, 120.5, 71.5, 33.5, 29.4, 21.3, 16.0, 14.0; HRMS (ESI) calcd for $\text{C}_{23}\text{H}_{26}\text{O}_4\text{S}$ ($\text{M} + \text{H}$) $^+$ 399.1625, found 399.1629.

4.1.6. (E)-3-(4-(2-hydroxyethoxy)-3,5-dimethylphenyl)-1-(4-(methylthio)phenyl)prop-2-en-1-one (10)

To a solution of **17** (100 mg, 0.34 mmol) in anhydrous DMF (2 mL) were added 2-bromoethanol (125 mg, 1.00 mmol) and potassium carbonate (232 mg, 1.68 mmol). The solution was heated to 90 °C for 6 h, then the solution was diluted with water and extracted with ethyl acetate. The organic layers were combined, concentrated and purified by column chromatography to give compound **10** as a yellow solid (65 mg, yield 57%). ^1H NMR (400 MHz, DMSO- d_6) δ 8.12–8.06 (m, 2H), 7.80 (d, $J = 15.5$ Hz, 1H), 7.62 (d, $J = 15.5$ Hz, 1H), 7.56 (s, 2H), 7.42–7.37 (m, 2H), 4.91 (t, $J = 5.5$ Hz, 1H), 3.84–3.79 (m, 2H), 3.74–3.68 (m, 2H), 2.56 (s, 3H), 2.28 (s, 6H); ^{13}C NMR (100 MHz, DMSO- d_6) δ 187.8, 157.9, 145.4, 143.6, 133.9, 131.2, 130.0, 129.7, 129.0, 125.0, 120.5, 74.0, 60.5, 16.0, 14.0; HRMS (ESI) calcd for $\text{C}_{20}\text{H}_{22}\text{O}_3\text{S}$ ($\text{M} + \text{H}$) $^+$ 343.1362, found 343.1364.

4.1.7. (E)-2,6-dimethyl-4-(3-(4-(methylthio)phenyl)-3-oxoprop-1-en-1-yl)phenyl propylcarbamate (14)

To a solution of **17** (50 mg, 0.17 mmol) and triethylamine (4 μL , 0.03 mmol) in anhydrous CH₂Cl₂ (1.5 mL) was added propyl isocyanate (21 mg, 0.25 mmol). The mixture was stirred at room temperature for 5 h, then the solution was concentrated and purified by column chromatography to give compound **14** as a white solid (46 mg, yield 72%). ^1H NMR (400 MHz, CDCl₃) δ 7.99–7.90 (m, 2H), 7.72 (d, $J = 15.6$ Hz, 1H), 7.42 (d, $J = 15.6$ Hz, 1H), 7.36–7.27 (m, 4H), 5.21 (t, $J = 6.1$ Hz, 1H), 3.29–3.17 (m, 2H), 2.53 (s, 3H), 2.22 (s, 6H), 1.66–1.53 (m, 2H), 0.97 (t, $J = 7.4$ Hz, 3H); ^{13}C NMR (100 MHz, CDCl₃) δ 189.3, 153.8, 150.1, 145.6, 144.3, 134.6, 132.3, 132.0, 129.1, 128.8, 125.2, 121.3, 43.1, 23.3, 16.4, 14.9, 11.3; HRMS (ESI) calcd for $\text{C}_{22}\text{H}_{25}\text{NO}_3\text{S}$ ($\text{M} + \text{H}$) $^+$ 384.1628, found 384.1631.

4.1.8. (E)-3-(3,5-dimethyl-4-(3-morpholinopropoxy)phenyl)-1-(4-(methylthio)phenyl)prop-2-en-1-one (15)

To a solution of **17** (100 mg, 0.34 mmol) in anhydrous DMF (1 mL) were added 4-(3-chloropropyl)morpholine (110 mg, 0.67 mmol) and potassium carbonate (232 mg, 1.68 mmol). The solution was heated to 90 °C for 6 h, then the solution was diluted with water and extracted with ethyl acetate. The organic layers were combined, concentrated and purified by column chromatography to give compound **15** as a white solid (101 mg, yield 71%). ^1H NMR (400 MHz, CDCl₃) δ 8.00–7.86 (m, 2H), 7.71 (d, $J = 15.6$ Hz, 1H), 7.41 (d, $J = 15.6$ Hz, 1H), 7.34–7.27 (m, 4H), 3.84 (t, $J = 6.3$ Hz, 2H), 3.73 (t, $J = 4.7$ Hz, 4H), 2.59 (t, $J = 7.3$ Hz, 2H), 2.53 (s, 3H), 2.48 (t, $J = 4.7$ Hz, 4H), 2.30 (s, 6H), 2.05–1.95 (m, 2H); ^{13}C NMR (100 MHz, CDCl₃) δ 189.3, 158.3, 145.5, 144.6, 134.8, 131.8, 130.5, 129.3, 129.0, 125.2, 120.6, 70.3, 67.1, 55.5, 53.8, 27.5, 16.5, 15.0; HRMS (ESI) calcd for $\text{C}_{25}\text{H}_{31}\text{NO}_3\text{S}$ ($\text{M} + \text{H}$) $^+$ 426.2097, found 426.2101.

4.1.9. (E)-4-(3-(4-(methylthio)phenyl)-3-oxoprop-1-en-1-yl)benzoic acid (**18**)

To a solution of **1a** (366 mg, 2.20 mmol) in methanol (10 mL) was added 4-formylbenzoic acid **2d** (300 mg, 2.00 mmol), followed by 40% sodium hydroxide solution (4 mL). The mixture was stirred at room temperature for 24 h. Subsequently, the solution was adjusted to pH = 2 and then the precipitate was filtered, washed with methanol and dried to give compound **18** as a yellow solid (415 mg, yield 70%). ¹H NMR (400 MHz, DMSO-*d*₆) δ 8.14–8.10 (m, 2H), 8.03 (d, *J* = 15.6 Hz, 1H), 8.00–7.97 (m, 4H), 7.76 (d, *J* = 15.6 Hz, 1H), 7.47–7.35 (m, 2H), 2.56 (s, 3H); ¹³C NMR (100 MHz, DMSO-*d*₆) δ 187.9, 167.2, 145.9, 142.4, 138.4, 133.6, 129.7, 129.2, 128.8, 125.0, 123.8, 14.0; HRMS (ESI) calcd for C₁₇H₁₄O₃S (M + H)⁺ 299.0736, found 299.0740.

4.1.10. (E)-3-(4-hydroxy-3,5-dimethylphenyl)-1-(4-(methylsulfinyl)phenyl)prop-2-en-1-one (**33**)

3-Chloroperbenzoic acid (m-CPBA) (289 mg, 1.68 mmol) was slowly added to the solution of **17** (500 mg, 1.68 mmol) in anhydrous CH₂Cl₂ (15 mL) under stirring at 0 °C. The mixture was stirred at room temperature for 5 h, then the solution was filtered and the filter cake was purified by column chromatography to obtain compound **33** as a yellow solid (354 mg, yield 67%). ¹H NMR (400 MHz, DMSO-*d*₆) δ 8.99 (s, 1H), 8.31–8.25 (m, 2H), 7.87–7.82 (m, 2H), 7.73 (d, *J* = 15.5 Hz, 1H), 7.65 (d, *J* = 15.5 Hz, 1H), 7.50 (s, 2H), 2.81 (s, 3H), 2.21 (s, 6H); ¹³C NMR (100 MHz, DMSO-*d*₆) δ 188.4, 156.6, 151.0, 145.7, 139.8, 129.9, 129.1, 125.6, 124.7, 123.9, 118.2, 43.1, 16.6; HRMS (ESI) calcd for C₁₈H₁₈O₃S (M + H)⁺ 315.1049, found 315.1051.

4.1.11. (E)-3-(4-hydroxy-3,5-dimethylphenyl)-1-(4-(methylsulfonyl)phenyl)prop-2-en-1-one (**34**)

3-Chloroperbenzoic acid (m-CPBA) (754 mg, 4.37 mmol) was slowly added to the solution of **17** (500 mg, 1.68 mmol) in anhydrous CH₂Cl₂ (15 mL) under stirring. The mixture was stirred at room temperature for 5 h, then the solution was filtered and the filter cake was purified by column chromatography to obtain compound **34** as a yellow solid (338 mg, yield 61%). ¹H NMR (400 MHz, DMSO-*d*₆) δ 8.38–8.27 (m, 2H), 8.15–8.02 (m, 2H), 7.72 (d, *J* = 15.6 Hz, 1H), 7.66 (d, *J* = 15.6 Hz, 1H), 7.52 (s, 2H), 3.31 (s, 3H), 2.20 (s, 6H); ¹³C NMR (100 MHz, DMSO-*d*₆) δ 188.4, 156.9, 146.4, 143.9, 142.0, 130.1, 129.3, 127.5, 125.5, 124.8, 118.1, 43.4, 16.7; HRMS (ESI) calcd for C₁₈H₁₈O₄S (M + H)⁺ 331.0999, found 331.0996.

4.1.12. Reaction analogues with glutathione

To a solution of each test compound (0.01 mmol) in DMSO (3.3 mL) and D-PBS (1.7 mL) was added GSH (0.20 mmol). The mixture was stirred at 37 °C. The course of reaction was monitored by HPLC at different time intervals.

4.2. Biology

4.2.1. Cell culture and stimulation

The murine macrophage cell line J774A.1 was purchased from Guangzhou Jennio Biotech Co., Ltd (China). J774A.1 cells were cultured in Dulbecco's Modified Eagle Medium (DMEM) (HyClone, USA) supplemented with 10% fetal bovine serum (FBS) (Gibco, USA) at 37 °C with 5% CO₂. Mouse bone marrow-derived macrophages (BMDMs) were collected from mice tibia and femoral bone marrow and cultured in RPMI 1640 medium with 10% FBS, 1 mM Penicillin-Streptomycin solution, 1 mM GlutaMax and 20 ng/mL M-CSF. For NLRP3 inflammasome activation, macrophages primed with 1 μg/mL LPS (Sigma-Aldrich, USA) for 5 h and treated with compounds for 1 h, and then the cells were stimulated with 10 μM nigericin (Invitrogen, USA) for 1 h. For NLR4 or AIM2 inflammasome

activation, J774A.1 cells were stimulated for 5 h with 1 μg/mL LPS and treatment for 1 h with compounds, and then the cells were infected for 4 h with FLA-ST Ultrapure (2.5 μg/mL) (Invitrogen, USA) or cells were transfected with poly (dA:dT) (0.25 μg/mL) (Invitrogen, USA) for 4 h using Lipofectamine 3000 (Invitrogen, USA).

4.2.2. Enzyme-linked immunosorbent assay

Supernatants from cell culture, peritoneal fluid, serum or colon homogenates were analyzed for mouse IL-1β (Invitrogen, USA) according to the manufacturer's instructions.

4.2.3. Cell viability assessment by CCK-8 assay

Cells were cultured in 96-well plates and grown to 80%–90% confluence, and pretreated with compounds for 24 h at 37 °C with 5% CO₂, then 10 μL/well CCK8 reagent was added for 1 h at 37 °C with 5% CO₂. Absorbance was measured using an Epoch 2 Microplate Reader at 450 nm (BioTek Instruments, Inc., Winooski, VT, USA).

4.2.4. Pyroptosis detection

J774A.1 cells were stimulated as usual, the cells supernatants were evaluated for LDH release using LDH detection kit (Beyotime, China) according to the manufacturer's protocol.

4.2.5. Western blotting analysis

Cells samples were lysed in RIPA Lysis Buffer (Beyotime, China) with protease inhibitors for 30 min at 4 °C. The proteins in lysate or supernatants were separated by 12% SDS-polyacrylamide gel, transferred to PVDF membrane, and hybridized with antibodies. Immunoreactive bands were detected by ECL (ThermoFisher Scientific, USA). Anti-mouse IL-1β (p17; cat# AF-401-NA) was from R&D Systems (USA). Anti-mouse caspase-1 (p20; cat# AG-20B-0042), anti-NLRP3 (cat# AG-20B-0014) and anti-ASC (cat# AG-25B-0006) were from AdipoGen (USA). Anti-β-actin (cat# P30002) was bought from Abmart (China). HRP Conjugated anti-Rabbit IgG (H + L) (cat# W4011), HRP Conjugated anti-Mouse IgG (H + L) (cat# W4021), and HRP Conjugated Donkey Anti-Goat IgG (cat# V8051) were bought from Promega (USA).

4.2.6. MitoSOX red label

After being stimulated as normal, J774A.1 cells were loaded with 5 μM MitoSOX Red (mitochondrial superoxide indicator) in the dark for 30 min at 37 °C. The fluorescence intensity was measured using a microplate reader Ex/Em = 510/580 nm. All data was obtained from experiments with at least three replicates.

4.2.7. Intracellular ROS detection

The total ROS in cells was detected by DCFH-DA assay or Muse Oxidative stress kit. The Cells plated in a 96-well black plate were stimulated as usual, and then the cells were incubated with 20 μM DCFH-DA (Sigma-Aldrich, USA) at 37 °C for 30 min. The fluorescence intensity was measured by a fluorescence microplate reader at 485 nm for excitation and 528 nm for emission. For muse detection, the cells were harvested and probed with 10 μM dihydroethidium (DHE (Abmart, China)) for 30 min at 37 °C in the dark. The fluorescence intensity of the Cells was analyzed by a Muse Cell Analyzer (Merck Millipore, Germany). All data were analyzed in at least three experiments.

4.2.8. Animal experiments

All animal experiments were performed according to the Guidelines for the Care and Use of Laboratory Animals and were approved by the Ethics Committee of Guangzhou Medical University (NO. 2020035). Animal studies are reported in compliance with the ARRIVE guidelines. All animals were raised under a 12 h light/dark cycle at 24 ± 1 °C with free access to food and water.

4.2.8.1. Induction of sepsis and drug treatments. Female C57BL/6 mice (6–8 weeks, $n = 6$ per group) were injected intraperitoneally with LPS (20 mg/kg) in the presence or absence of compound **40** (pre-treat orally 3 days, 25 mg/kg/day and 100 mg/kg/day). After 6 h, the serum samples and peritoneal fluid were collected to tested to tested the secretion of IL-1 β by ELISA.

4.2.8.2. Induction of colitis and drug treatments. Male C57BL/6 mice (6–8 weeks, $n = 5$ per group) were treated with 2% DSS in distilled water for 7 consecutive days. The test compound **40** was administered orally (25 mg/kg/day and 100 mg/kg/day) for 10 consecutive days, starting 3 days before colitis induction. Body weight and the presence of gross blood in feces were monitored daily. The macroscopic score was evaluated on the colon, while biochemical assays were performed on colon specimens.

Declaration of competing interest

The authors declare that they have no known competing financial interests or personal relationships that could have appeared to influence the work reported in this paper.

Acknowledgments

This work was supported by the National Natural Science Foundation of China (NSFC) (NO. 81803364 to Z. Yang and NO. 81872743 to W. Hu).

Appendix A. Supplementary data

Supplementary data to this article can be found online at <https://doi.org/10.1016/j.ejmech.2021.113417>.

References

- [1] M.S.J. Mangan, E.J. Olhava, W.R. Roush, H.M. Seidel, G.D. Glick, E. Latz, Targeting the NLRP3 inflammasome in inflammatory diseases, *Nat. Rev. Drug Discov.* 17 (2018) 588–606.
- [2] E. Latz, T.S. Xiao, A. Stutz, Activation and regulation of the inflammasomes, *Nat. Rev. Immunol.* 13 (2013) 397–411.
- [3] E.-K. Jo, J.K. Kim, D.-M. Shin, C. Sasakawa, Molecular mechanisms regulating NLRP3 inflammasome activation, *Cell. Mol. Immunol.* 13 (2016) 148–159.
- [4] T. Próchnicki, M.S. Mangan, E. Latz, Recent insights into the molecular mechanisms of the NLRP3 inflammasome activation, *Front. Immunol.* 5 (2016) 1469.
- [5] A. Malik, T.-D. Kanneganti, Inflammasome activation and assembly at a glance, *J. Cell Sci.* 130 (2017) 3955–3963.
- [6] D. Sharma, T.-D. Kanneganti, The cell biology of inflammasomes: mechanisms of inflammasome activation and regulation, *J. Cell Biol.* 213 (2016) 617–629.
- [7] Y. He, H. Hara, G. Núñez, Mechanism and regulation of NLRP3 inflammasome activation, *Trends Biochem. Sci.* 41 (2016) 1012–1021.
- [8] D. De Nardo, E. Latz, NLRP3 inflammasomes link inflammation and metabolic disease, *Trends Immunol.* 32 (2011) 373–379.
- [9] C. Bauer, P. Duewell, C. Mayer, H.A. Lehr, K.A. Fitzgerald, M. Dauer, J. Tschoop, S. Endres, E. Latz, M. Schnurr, Colitis induced in mice with dextran sulfate sodium (DSS) is mediated by the NLRP3 inflammasome, *Gut* 59 (2010) 1192–1199.
- [10] Y. Zhen, H. Zhang, NLRP3 inflammasome and inflammatory bowel disease, *Front. Immunol.* 10 (2019) 276.
- [11] A.R. Mridha, A. Wree, A.A.B. Robertson, M.M. Yeh, C.D. Johnson, D.M. Van Rooyen, F. Haczezy, N.C.-H. Teoh, C. Savard, G.N. Ioannou, S.L. Masters, K. Schroder, M.A. Cooper, A.E. Feldstein, G.C. Farrell, NLRP3 inflammasome blockade reduces liver inflammation and fibrosis in experimental NASH in mice, *J. Hepatol.* 66 (2017) 1037–1046.
- [12] H. Thomas, NAFLD: a critical role for the NLRP3 inflammasome in NASH, *Nat. Rev. Gastroenterol. Hepatol.* 14 (2017) 197.
- [13] J.G. Walsh, D.A. Muruve, C. Power, Inflammasomes in the CNS, *Nat. Rev. Neurosci.* 15 (2014) 84–97.
- [14] M.T. Heneka, M.P. Kummer, A. Stutz, A. Delekate, S. Schwartz, A. Vieira-Saecker, A. Griep, D. Axt, A. Remus, T.-C. Tzeng, E. Gelpi, A. Halle, M. Korte, E. Latz, D.T. Golenbock, NLRP3 is activated in Alzheimer's disease and contributes to pathology in APP/PS1 mice, *Nature* 493 (2013) 674–678.
- [15] M. Saresella, F. La Rosa, F. Piancone, M. Zoppis, I. Marventano, E. Calabrese, V. Rainone, R. Nemni, R. Mancuso, M. Clerici, The NLRP3 and NLRP1 inflammasomes are activated in Alzheimer's disease, *Mol. Neurodegener.* 11 (2016) 23.
- [16] R. Muñoz-Planillo, P. Kuffa, G. Martínez-Colón, B.L. Smith, T.M. Rajendiran, G. Núñez, K⁺ efflux is the common trigger of NLRP3 inflammasome activation by bacterial toxins and particulate matter, *Immunity* 38 (2013) 1142–1153.
- [17] V. Hornung, F. Bauernfeind, A. Halle, E.O. Samstad, H. Kono, K.L. Rock, K.A. Fitzgerald, E. Latz, Silica crystals and aluminum salts activate the NALP3 inflammasome through phagosomal destabilization, *Nat. Immunol.* 9 (2008) 847–856.
- [18] J. Dan Dunn, L.A. Alvarez, X. Zhang, T. Soldati, Reactive oxygen species and mitochondria: a nexus of cellular homeostasis, *Redox Biol* 6 (2015) 472–485.
- [19] B.F. Py, M.-S. Kim, H. Vakifahmetoglu-Norberg, J. Yuan, Deubiquitination of NLRP3 by BRCC3 critically regulates inflammasome activity, *Mol. Cell.* 49 (2013) 331–338.
- [20] R.C. Coll, A.A.B. Robertson, J.J. Chae, S.C. Higgins, R. Muñoz-Planillo, M.C. Inerra, I. Vetter, L.S. Dungan, B.G. Monks, A. Stutz, D.E. Croker, M.S. Butler, M. Haneklaus, C.E. Sutton, G. Núñez, E. Latz, D.L. Kastner, K.H.G. Mills, S.L. Masters, K. Schroder, M.A. Cooper, L.A.J. O'Neill, A small-molecule inhibitor of the NLRP3 inflammasome for the treatment of inflammatory diseases, *Nat. Med.* 21 (2015) 248–255.
- [21] C. Marchetti, B. Swartzwelter, F. Gamboni, C.P. Neff, K. Richter, T. Azam, S. Carta, I. Tengesdal, T. Nemkov, A. D'Alessandro, C. Henry, G.S. Jones, S.A. Goodrich, J.P. St Laurent, T.M. Jones, C.L. Scribner, R.B. Barrow, R.D. Altman, D.B. Skouras, M. Gattorno, V. Grau, S. Janciauskiene, A. Rubartelli, L.A.B. Joosten, C.A. Dinarello, OLT1177, a β -sulfonyl nitrile compound, safe in humans, inhibits the NLRP3 inflammasome and reverses the metabolic cost of inflammation, *Proc. Natl. Acad. Sci. U.S.A.* 115 (2018) 1530–1539.
- [22] C. Juliana, T. Fernandes-Alnemri, J. Wu, P. Datta, L. Solorzano, J.-W. Yu, R. Meng, A.A. Quong, E. Latz, C.P. Scott, E.S. Alnemri, Anti-inflammatory compounds parthenolide and Bay 11-7082 are direct inhibitors of the inflammasome, *J. Biol. Chem.* 285 (2010) 9792–9802.
- [23] M. Cocco, C. Pellegrini, H. Martínez-Banaclocha, M. Giorgis, E. Marini, A. Costale, G. Miglio, M. Fornai, L. Antonioli, G. López-Castejón, A. Tapia-Abellán, D. Angosto, I. Hafner-Bratkovič, L. Regazzoni, C. Blandizzi, P. Pelegrin, M. Bertinaria, Development of an acrylate derivative targeting the NLRP3 inflammasome for the treatment of inflammatory bowel disease, *J. Med. Chem.* 60 (2017) 3656–3671.
- [24] Y. Ou, P. Sun, N. Wu, H. Chen, D. Wu, W. Hu, Z. Yang, Synthesis and biological evaluation of parthenolide derivatives with reduced toxicity as potential inhibitors of the NLRP3 inflammasome, *Bioorg. Med. Chem. Lett* 30 (2020) 127399.
- [25] Y. Jiang, L. He, J. Green, H. Blevins, C. Guo, S.H. Patel, M.S. Halquist, M. McRae, J. Venitz, X.-Y. Wang, S. Zhang, Discovery of second-generation NLRP3 inflammasome inhibitors: design, synthesis, and biological characterization, *J. Med. Chem.* 62 (2019) 9718–9731.
- [26] W. Deng, Z. Yang, H. Yue, Y. Ou, W. Hu, P. Sun, Disulfiram suppresses NLRP3 inflammasome activation to treat peritoneal and gouty inflammation, *Free Radic. Biol. Med.* 152 (2020) 8–17.
- [27] H. Jiang, H. He, Y. Chen, W. Huang, J. Cheng, J. Ye, A. Wang, J. Tao, C. Wang, Q. Liu, T. Jin, W. Jiang, X. Deng, R. Zhou, Identification of a selective and direct NLRP3 inhibitor to treat inflammatory disorders, *J. Exp. Med.* 214 (2017) 3219–3238.
- [28] C. Guo, J.W. Fulp, Y. Jiang, X. Li, J.E. Chojnacki, J. Wu, X.-Y. Wang, S. Zhang, Development and characterization of a hydroxyl-sulfonamide analogue, 5-chloro-N-[2-(4-hydroxysulfamoyl-phenyl)-ethyl]-2-methoxy-benzamide, as a novel NLRP3 inflammasome inhibitor for potential treatment of multiple sclerosis, *ACS Chem. Neurosci.* 8 (2017) 2194–2201.
- [29] A.G. Schwaib, K.B. Spencer, Strategies for targeting the NLRP3 inflammasome in the clinical and preclinical space, *J. Med. Chem.* 64 (2021) 101–122.
- [30] B. Staels, A. Rubenstrunk, B. Noel, G. Rigou, P. Delataille, L.J. Millatt, M. Baron, A. Lucas, A. Tailleux, D.W. Hum, V. Ratziu, B. Cariou, R. Hanf, Hepatoprotective effects of the dual peroxisome proliferator-activated receptor α /delta agonist, GFT505, in rodent models of nonalcoholic fatty liver disease/nonalcoholic steatohepatitis, *Hepatology* 58 (2013) 1941–1952.
- [31] V. Ratziu, S.A. Harrison, S. Francque, P. Bedossa, P. Leher, L. Serfaty, M. Romero-Gomez, J. Boursier, M. Abdelmalek, S. Caldwell, J. Drenth, Q.M. Anstee, D. Hum, R. Hanf, A. Roudot, S. Megnier, B. Staels, A. Sanyal, Elafibranor, an agonist of the peroxisome proliferator-activated receptor- α and - δ , induces resolution of nonalcoholic steatohepatitis without fibrosis worsening, *Gastroenterology* 150 (2016) 1147–1159.
- [32] P.D. Leeson, Molecular inflation, attrition and the rule of five, *Adv. Drug Deliv. Rev.* 101 (2016) 22–33.
- [33] M.D. Shultz, Two decades under the influence of the rule of five and the changing properties of approved oral drugs, *J. Med. Chem.* 62 (2019) 1701–1714.
- [34] C. Abad-Zapatero, J.T. Metz, Ligand efficiency indices as guideposts for drug discovery, *Drug Discov. Today* 10 (2005) 464–469.
- [35] A.B. Reitz, G.R. Smith, B.A. Tounge, C.H. Reynolds, Hit triage using efficiency indices after screening of compound libraries in drug discovery, *Curr. Top. Med. Chem.* 9 (2009) 1718–1724.
- [36] P.D. Leeson, B. Springthorpe, The influence of drug-like concepts on decision-making in medicinal chemistry, *Nat. Rev. Drug Discov.* 6 (2007) 881–890.
- [37] A. Tarcsay, K. Nyiri, G.M. Keseru, Impact of lipophilic efficiency on compound quality, *J. Med. Chem.* 55 (2012) 1252–1260.
- [38] M.H. Potashman, M.E. Duggan, Covalent modifiers: an orthogonal approach to

- drug design, *J. Med. Chem.* 52 (2009) 1231–1246.
- [39] T. Barf, A. Kaptein, Irreversible protein kinase inhibitors: balancing the benefits and risks, *J. Med. Chem.* 55 (2012) 6243–6262.
- [40] K.-D. Wu, G.S. Chen, J.-R. Liu, C.-E. Hsieh, J.-W. Chern, Acrylamide functional group incorporation improves drug-like properties: an example with EGFR inhibitors, *ACS Med. Chem. Lett.* 10 (2019) 22–26.
- [41] S. De Cesco, J. Kurian, C. Dufresne, A.K. Mittermaier, N. Moitessier, Covalent inhibitors design and discovery, *Eur. J. Med. Chem.* 138 (2017) 96–114.
- [42] D.K. Mahapatra, S.K. Bharti, V. Asati, Chalcone derivatives: anti-inflammatory potential and molecular targets perspectives, *Curr. Top. Med. Chem.* 17 (2017) 3146–3169.
- [43] A. Rolt, L.S. Cox, Structural basis of the anti-ageing effects of polyphenolics: mitigation of oxidative stress, *BMC Chem* 14 (2020) 50.
- [44] C. Zhuang, W. Zhang, C. Sheng, W. Zhang, C. Xing, Z. Miao, Chalcone: a privileged structure in medicinal chemistry, *Chem. Rev.* 117 (2017) 7762–7810.
- [45] D.D. Eichele, K.K. Kharbanda, Dextran sodium sulfate colitis murine model: an indispensable tool for advancing our understanding of inflammatory bowel diseases pathogenesis, *World J. Gastroenterol.* 23 (2017) 6016–6029.
- [46] J. Xie, L. Li, S. Deng, J. Chen, Q. Gu, H. Su, L. Wen, S. Wang, C. Lin, C. Qi, Q. Zhang, J. Li, X. He, W. Li, L. Wang, L. Zheng, Slit 2/Robo 1 mitigates DSS-induced ulcerative colitis by activating autophagy in intestinal stem cell, *Int. J. Biol. Sci.* 16 (2020) 1876–1887.